

Article

Distribution and Meteorological Control of PM_{2.5} and Its Effect on Visibility in Northern Thailand

Teerachai Amnuaylojaroen ^{1,2,*} , Phonwilai Kaewkanchanawong ¹ and Phatcharamon Panpeng ¹

¹ Department of Environmental Science, School of Energy and Environment, University of Phayao, Phayao 56000 1, Thailand

² Atmospheric Pollution and Climate Research Unit, School of Energy and Environment, University of Phayao, Phayao 56000 2, Thailand

* Correspondence: teerachai4@gmail.com or teerachai.am@up.ac.th

Abstract: In the dry season, the north of Thailand always experiences reduced air quality, reduced visibility, and public health exposure from the burning of biomass domestically and in surrounding countries. The purpose of this research was to investigate the distribution and the meteorological control of PM_{2.5} accumulation, as well as its effect on visibility in northern Thailand in 2020. The Geographic Information System (GIS) was applied for the analysis of the spatial distribution, while Pearson's correlation coefficient was utilized to examine the association between PM_{2.5} and meteorological variables. The results showed that the PM_{2.5} concentrations were in the range of 16–195 µg/m³ in 2020. The high level of PM_{2.5} in Lampang, Chiang Rai, and Chiang Mai provinces was in the range of 150 to 195 µg/m³ from January to May. Favorable meteorological conditions included low wind and relative humidity, and high temperatures contributed to high PM_{2.5} concentrations in northern Thailand. Domestic burning and burning in neighboring countries contribute to huge amounts of smoke that cause low visibility in northern Thailand, especially at 1 km above ground level, with a reduced visibility in the range of 70–90% for all provinces in April.

Keywords: PM_{2.5}; PM_{2.5} meteorology; visibility; air quality; northern Thailand



Citation: Amnuaylojaroen, T.; Kaewkanchanawong, P.; Panpeng, P. Distribution and Meteorological Control of PM_{2.5} and Its Effect on Visibility in Northern Thailand. *Atmosphere* **2023**, *14*, 538. <https://doi.org/10.3390/atmos14030538>

Academic Editor: Mark C. Green

Received: 21 February 2023

Revised: 7 March 2023

Accepted: 10 March 2023

Published: 11 March 2023



Copyright: © 2023 by the authors. Licensee MDPI, Basel, Switzerland. This article is an open access article distributed under the terms and conditions of the Creative Commons Attribution (CC BY) license (<https://creativecommons.org/licenses/by/4.0/>).

1. Introduction

In Southeast Asia, agricultural wastes are eliminated by crop management through the use of fires as well as deforestation for cropland [1,2]. This normally happens during the dry season, around November to April, as a result of extensive fire emissions at the onset of the Asian summer monsoon [3,4]. Simultaneously, a layer of temperature inversion from high pressure is present in many Southeast Asian countries, such as Thailand, Laos, and Burma, which, in conjunction with the increasing fire activity, contributes to the air quality problem in this region [3]. Previous studies have demonstrated that fire emission is the primary factor influencing ambient air quality in Mainland Southeast Asia, particularly for particulate matter with an aerodynamic width of less than 2.5 µm (PM_{2.5}) [3,5].

Air pollution from biomass burning is a common occurrence in northern Thailand, which is located in the north of the peninsula of Southeast Asia. This is particularly apparent from January to April [3]. Concerns regarding the region's air quality are made worse by the large amount of biomass emissions coming from domestic sources and nearby countries including Burma, Laos, Vietnam, and Cambodia [6,7]. Furthermore, the problem of air pollution in northern Thailand is probably dominated by a mix of meteorological and geographic factors. Weather conditions that exacerbate particle matter building, burning of stubble in advance of impending rain and crop planting, and the multiple areas in northern Thailand's narrow hills that serve as desirable basins for air pollutants all contribute to air pollution [8,9].

In order to properly assess and manage PM_{2.5} pollution, it is crucial to quantify the main contributing factors. According to previous research [10,11], weather factors can

considerably disperse, remove, and induce pollutants as well as exert an influence on long-term variations in $PM_{2.5}$. As a result, the distribution of $PM_{2.5}$ is largely determined by weather patterns [12]. To support the government and policymakers in managing air quality, several previous studies have suggested a forecasting model for $PM_{2.5}$ based on the association between meteorological factors and particulate matter. For example, Akbal and Ünlü [13] revealed the use of an advanced deep learning approach to expand understanding of particulate matter prediction by applying advanced machine learning with several trained methodologies, including Gaussian process regression, random forest regression (FRF), two different types of support vector machines (SVM), and artificial neural networks (ANN), which used meteorological factors as explanatory variables to predict $PM_{2.5}$ [14]. Based on ANN along with k-mean clustering, principal component analysis (PCA) that contains wind speed and direction, temperature, precipitation, relative humidity, and solar radiation is also performed to forecast $PM_{2.5}$ [15]. A hybrid deep learning method that includes the coupling of wavelet transformation and ANN with different structures and several meteorological data points including temperature, wind direction, and humidity also had good performance in forecasting $PM_{2.5}$ [16]. As such, Akdi et al. [17] recently developed harmonic regression (HR), which is a univariate time series modeling approach that has advantages over classical time series approaches.

Low atmospheric visibility, which is a direct result of high-level particulate accumulation, provides the public with the clearest understanding of air quality, and it has been typically utilized as a surrogate for pollutant concentrations during times and in places where there were no monitoring systems for air quality [18]. For instance, severe air pollution was recently characterized by haze weather, which is described as an atmospheric occurrence with horizontal visibility less than 10 km caused by the dispersion of huge fine particles [19]. Both the general public and the scientific community were very concerned about this phenomenon [20–22]. Studies conducted in the past have investigated the relationship between meteorological variables and ambient air pollution. For instance, Yang et al. [21] determined that weather-related factors were responsible for 1.8 of the 15 $\mu\text{g}/\text{m}^3/\text{decade}$ variation in $PM_{2.5}$ in the east of China between 1985 and 2005. According to a study by Zhang et al. [23], between 2013 and 2017 the proportionate contribution of climatic factors to large polluting events in the Beijing–Tianjin–Hebei region was stronger than 50%. Many studies have also attempted to establish a connection between $PM_{2.5}$ and atmospheric visibility [24,25]. Due to geographical variations in air pollution and meteorological conditions as well as various analytic techniques, these earlier investigations, which were primarily conducted in a single city, have showed conflicting results. Therefore, in order to fill these information gaps, a study on the impact of $PM_{2.5}$ on visibility was performed in multiple cities in northern Thailand throughout a haze episode. Furthermore, relationships between meteorological factors, such as relative humidity, surface temperature, wind speed, and $PM_{2.5}$, were studied to improve the understanding of those patterns during the haze period in northern Thailand.

2. Materials and Methods

To analyze $PM_{2.5}$ pollution and its effect on visibility in northern Thailand, several datasets, including ground-based measurements from the Pollution Control Department (PCD) in northern Thailand, the aerosol optical depth (AOD) data from Modern-Era Retrospective Analysis for Research and Applications version 2 (MERRA-2), and satellite images from both the Visible Infrared Imaging Radiometer Suite (VIIRS) of the National Oceanic and Atmospheric Administration (NOAA)-20 and the VIIRS-National Polar Partnership (NPP) were used for the analysis. The Pearson correlation was applied to analyze the relationship between $PM_{2.5}$ and meteorological factors using data from the ground-based measurement of PCD in northern Thailand. Spatial analysis of $PM_{2.5}$ and AOD was performed by Geographical Information System (GIS)-based Inverse Distance Weighted (IDW) interpolation.

2.1. Study Area and Air Pollution Data

We acquired hourly averaged pollution data from the Thai Pollution Control Department (PCD) in northern Thailand. Individual data were provided, including PM_{2.5}, temperature, wind speed, and relative humidity at 3 m. We only considered background monitors with just enough data (about 25% missing data [26]) to verify that they represented the full period. As a result, the quantity of monitors with sufficient data was reduced to seven, as indicated in Table 1. Figure 1 illustrates the seven urban ground-monitoring stations chosen for this study. The quality assurance and quality control (QA/QC) systems relied on protocols established by the United States Environmental Protection Agency (EPA) [27]. The sampling performance criterion required the collection of quantifiable data on all PM_{2.5} exposures and microenvironmental concentrations. QA was guided by the following principles: (1) all processes must be thoroughly designed, tested, and implemented in accordance with standard operating procedures approved by the research director; (2) all data must be easily traceable; and (3) any deviations and irregularities must be documented [27].

Table 1. Description of observation location from PCD in northern Thailand.

Name	Code	Latitude	Longitude
Chiang Mai Province Office, Chiang Mai	CM	18.84	98.96
Mae Sai, Chiang Rai	CR	20.42	99.88
Lampang Meteorological Office, Lampang	LP1	18.27	99.50
Sop Pat, Lampang Province	LP2	18.25	99.76
Muang, Lamphun Province	LPh	18.56	99.00
Muang, Nan Province	NAN1	18.78	100.77
Chaloemprakiat, Nan Province	NAN2	19.57	101.08

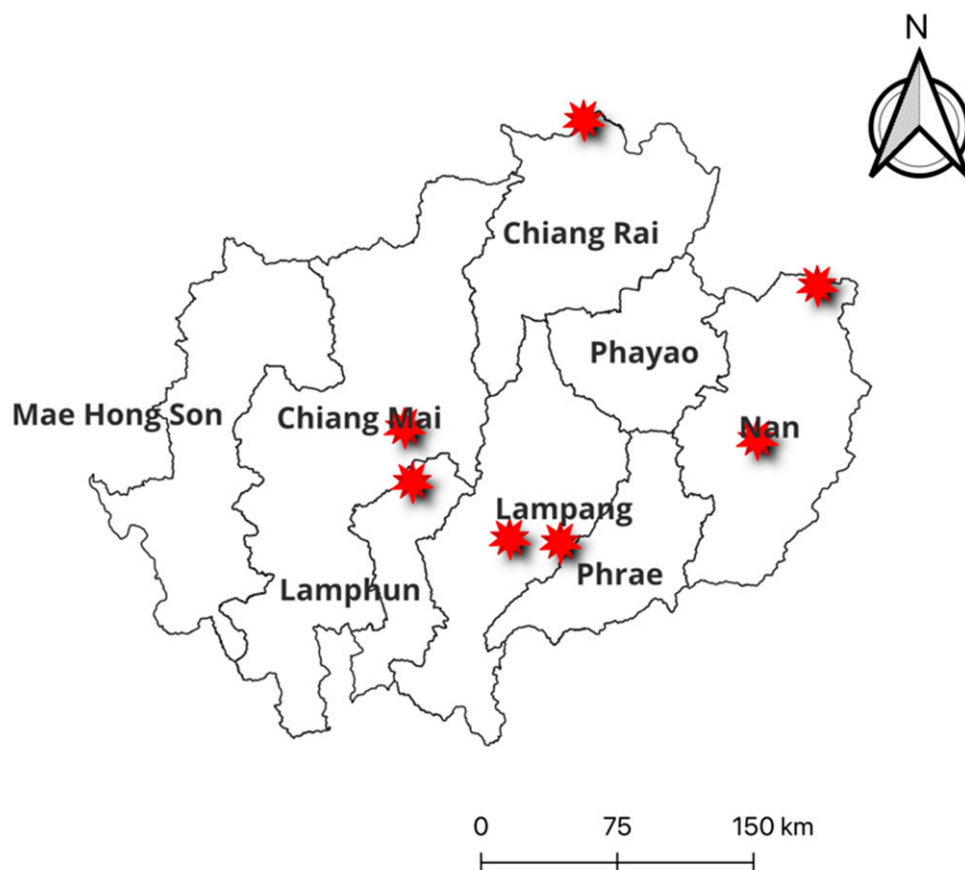


Figure 1. Map of northern Thailand demonstrating the monitoring stations (red stars).

2.2. Data Used

We used the aerosol optical depth (AOD) data from Modern-Era Retrospective analysis for Research and Applications version 2 (MERRA-2, M2IMNXGAS), which provide monthly mean data for this study. The data include an assimilation of both aerosol optical depth analysis increment and aerosol optical depth analysis. The data also contain the parameter variation. In addition, this dataset is the most recent version of global atmospheric reanalysis for the satellite that spans from 1980 to the present with a lag of approximately three weeks following the end of each month (https://disc.gsfc.nasa.gov/datasets/M2IMNXGAS_5.12.4/summary, accessed on 9 March 2023).

The Visible Infrared Imaging Radiometer Suite (VIIRS)—National Polar-orbiting Partnership (NPP) satellite image was utilized to determine the trajectory of the smoke plume in northern Thailand. This confluence of wavelengths is referred to as real color or natural color. The images depict land surface, sea, and atmospheric characteristics that appear natural. Only near real-time imagery of the Visible Infrared Imaging Radiometer Suite (VIIRS) Corrected Reflectance is available. The VIIRS sensor is on the Suomi National Polar-orbiting Partnership (NPP) satellite, which is a joint mission between NASA and NOAA. Worldview and the Global Imagery Browse Services can visualize the imagery (GIBS) with a resolution of 750 m and 375 m for M Bands and I Bands, respectively.

In this investigation, the satellite image of fire from VIIRS NOAA-20 was utilized. The Fire layer of the VIIRS displays active fire detection systems and heating anomalies. The layer of fire is important for investigating the distribution in terms of spatiality and temporality of fire, locating recurring hot spots, and identifying the air pollution source from a plume that may have negative health effects on humans. Sensor resolution is 375 m, picture resolution is 250 m, and temporal resolution is twice each day. The temperature anomalies are shown as red dots (approximate center of a 375 m pixel). The nominal observation times (equator crossover) for VIIRS S-NPP are 1:30 p.m. and 1:30 a.m., while NOAA-20 operates approximately 50 min ahead of S-NPP. Due to its polar orbit, mid-latitudes will receive three to four looks per day.

2.3. Data Analysis

To analyze the relationship between $PM_{2.5}$ and meteorological variables including wind speed, surface temperature, and relative humidity, the Pearson correlation coefficient in Equation (1) was utilized in this study.

$$r = \frac{n(\sum xy) - (\sum x)(\sum y)}{\sqrt{[n \sum x^2 - (\sum x)^2][n \sum y^2 - (\sum y)^2]}} \quad (1)$$

where r is correlation coefficient, while x and y represent values of the x and y variable in a sample.

The Pearson correlation coefficient (r) is a linear correlation coefficient that can be used to assess two or more correlated items. Due to the fact that it can indicate the degree of linear association between atmospheric parameters and air pollutants, it can serve as a measure of linearity. It can take values ranging from -1 to 1 . A perfect linear relationship ($r = -1$ or $r = 1$) means that one of the variables can be perfectly explained by a linear function of the other.

Meanwhile, spatial analysis was described using interpolated maps that were transformed to raster images (about 30 m resolution) and categorized to depict the distribution of the number of participants in the research area using inverse distance weighted classification (IDW). The IDW interpolation determines cell values by linearly weighting a series of sample points. The inverse distance determines the weight. The extrapolated surface might be that of a variable that is position-dependent. This method assumes that the effect of the factor being mapping reduces as one moves away from the sampled location. The parameters of the interpolated surface can also be changed by limiting the amount of input

points used in the calculation of each output cell value. By restricting the amount of input points analyzed, processing times can be reduced. Consider that input points located far from the cell location where the prediction is being made may have little or no spatial connection and so may be removed from the calculation [28,29].

The IDW approach, which is based on the concept of distance weighting, is utilized to interpolate spatial data in this study. This method is useful for estimating unknown depth data based on known (near) recorded depths. Equations (2) and (3) provide the IDW formulas:

$$R = \sum_{i=1}^N w_i R_i \quad (2)$$

$$w_i = \frac{d_i^\alpha}{\sum_{i=1}^N d_i^\alpha} \quad (3)$$

where R represents the unknown depth data (cm), R_i represents the depth data measured (cm), N is the number of points (in the search radius area), d_i is the distance from each depth to the calculated grid node, α is the power and is also a control parameter, generally assumed to be two, and w_i presents the weighting of each depth.

The visibility was estimated as follows (4), which is based on work by Baumer et al. [30]:

$$V_a = 3.912 (Z_i) AOD_{500}^{-1} \quad (4)$$

This approach also assumes that all aerosol is located within the mixing layer with a height of Z_i . Where V_a is the maximum horizontal distance that the human eye can see, Z_i is constant with values of 1.0, 1.5, and 3 km [31], and AOD_{500} is the AOD at 500 nm.

3. Results and Discussion

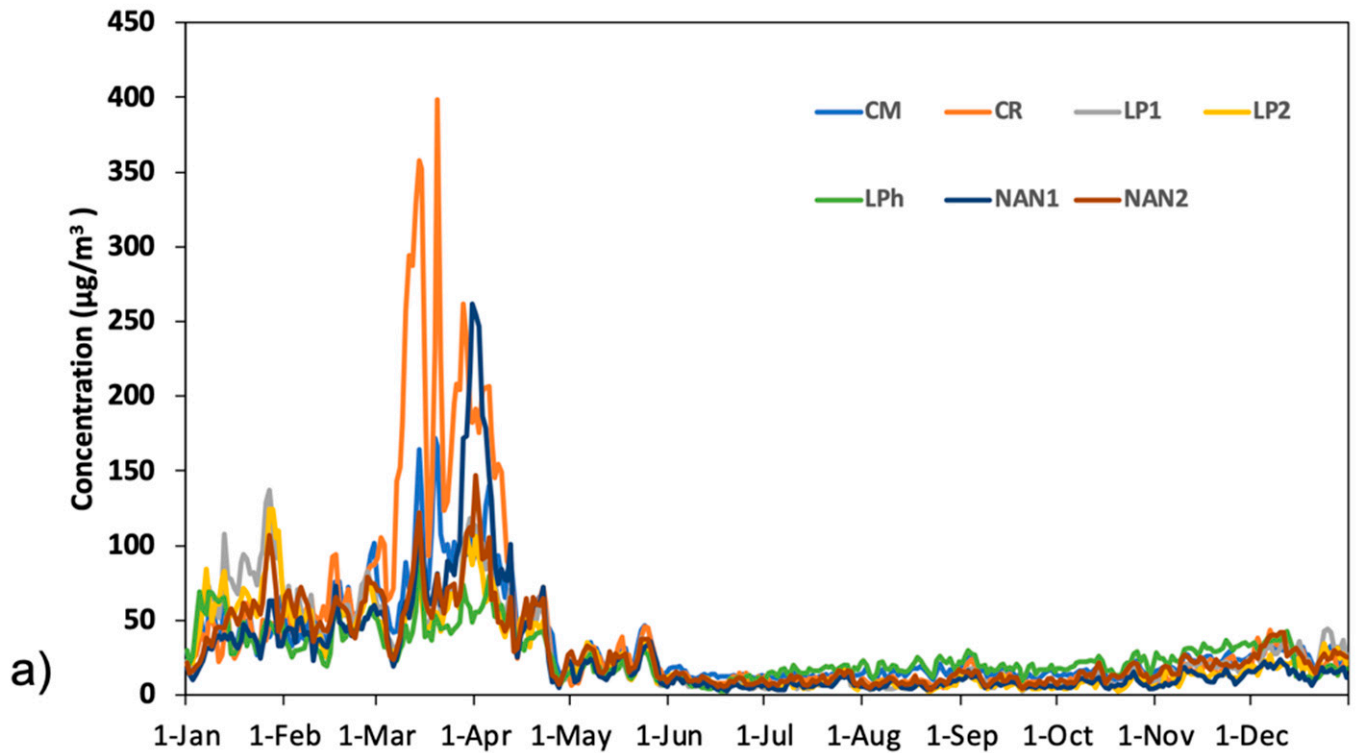
3.1. $PM_{2.5}$ Monitoring in Northern Thailand

Figure 2 illustrates the daily $PM_{2.5}$ concentrations in five provinces, including Chiang Mai, Chiang Rai, Lampang, Lamphun, and Nan in northern Thailand in 2020. The daily average of $PM_{2.5}$ concentrations was higher than both Thailand's and the USEPA's guidelines, particularly from January to May. The highest levels of $PM_{2.5}$ concentrations were found largely from March to April. The seasonal changes in emissions in this region are very certainly influenced by biomass burning [14,32]. When the $PM_{2.5}$ in the dry season (February and March) are investigated, the highest range of $PM_{2.5}$ concentration is revealed to be in the range of 100–200 $\mu\text{g}/\text{m}^3$. The high particulate pollution during dry season is likely due to extensive biomass burning from agricultural burning in preparation for rice planting season. Along with the long-range transport of air pollutants from neighboring countries such as Laos, Vietnam, and Burma induced by meteorological conditions, these factors contribute to the air pollution problem in northern Thailand [8].

3.2. Correlation between $PM_{2.5}$ and Meteorological Condition

Figure 3 shows the correlation between $PM_{2.5}$ and meteorological variables including relative humidity (RH), surface temperature (Temp), and wind speed (ws) during January and May 2020 in northern Thailand. The $PM_{2.5}$ concentration for all months was negatively related to relative humidity. Furthermore, a negative relationship was found between $PM_{2.5}$ and temperature in January, while a positive relationship was found in the other months. The $PM_{2.5}$ in most of the months was also negatively correlated with wind speed, while a negative relationship was found in March. The relationships of different air pollutants with wind speed and wind direction are illustrated in Figure 4. In general, dominant $PM_{2.5}$ concentrations originate from the southeast ($0\text{--}1 \text{ m}\cdot\text{s}^{-1}$). In March, high concentrations of $PM_{2.5}$ ($100 \mu\text{g}/\text{m}^3$ and above) originate from the southeast and west ($0\text{--}0.8 \text{ m}\cdot\text{s}^{-1}$), while the lowest concentration was found with the same wind direction when wind speeds were low ($0\text{--}0.5 \text{ m}\cdot\text{s}^{-1}$). These results reflect previous findings that high concentrations of $PM_{2.5}$ were mostly associated with low wind speed conditions and when weak winds prevail along the southeast [33,34] (Shelton et al., 2022; Hama et al., 2020).

Daily Mean PM2.5 Concentration, northern Thailand



Daily Mean PM2.5 Concentration during January - May, northern Thailand

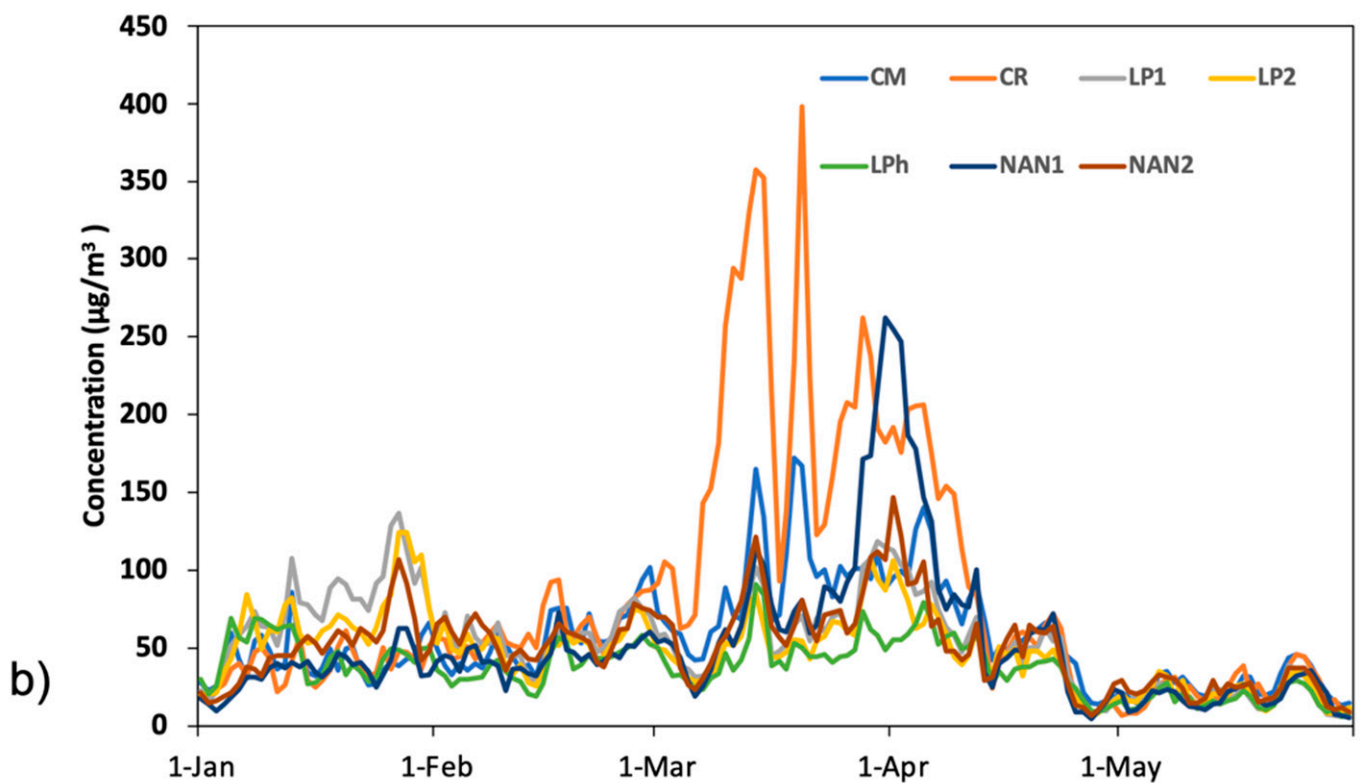


Figure 2. Daily mean observed PM_{2.5} concentrations at seven location sites in northern Thailand, (a) for the entire year 2020 and (b) during January and May 2020.

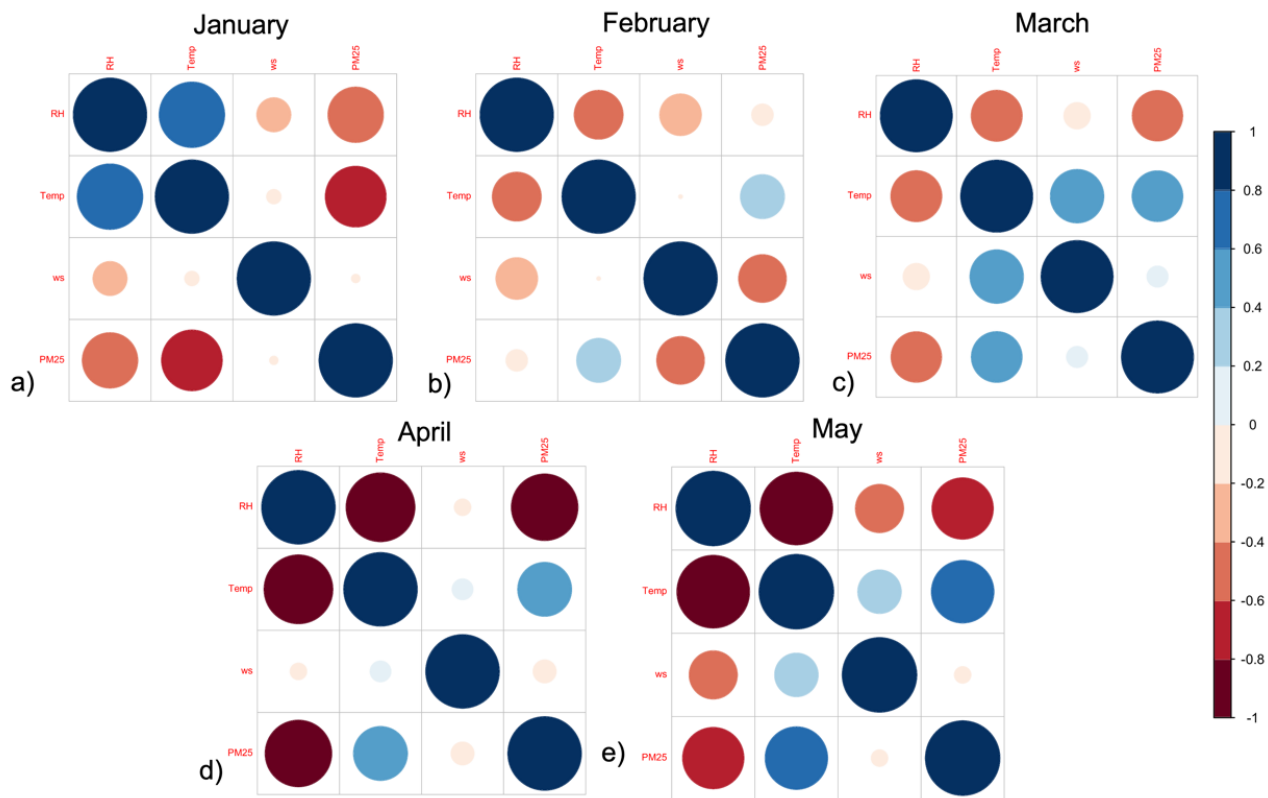


Figure 3. Corrplot for the monthly PM_{2.5}, and meteorological variables in (a) January, (b) February, (c) March, (d) April, and (e) May 2020 in northern Thailand.

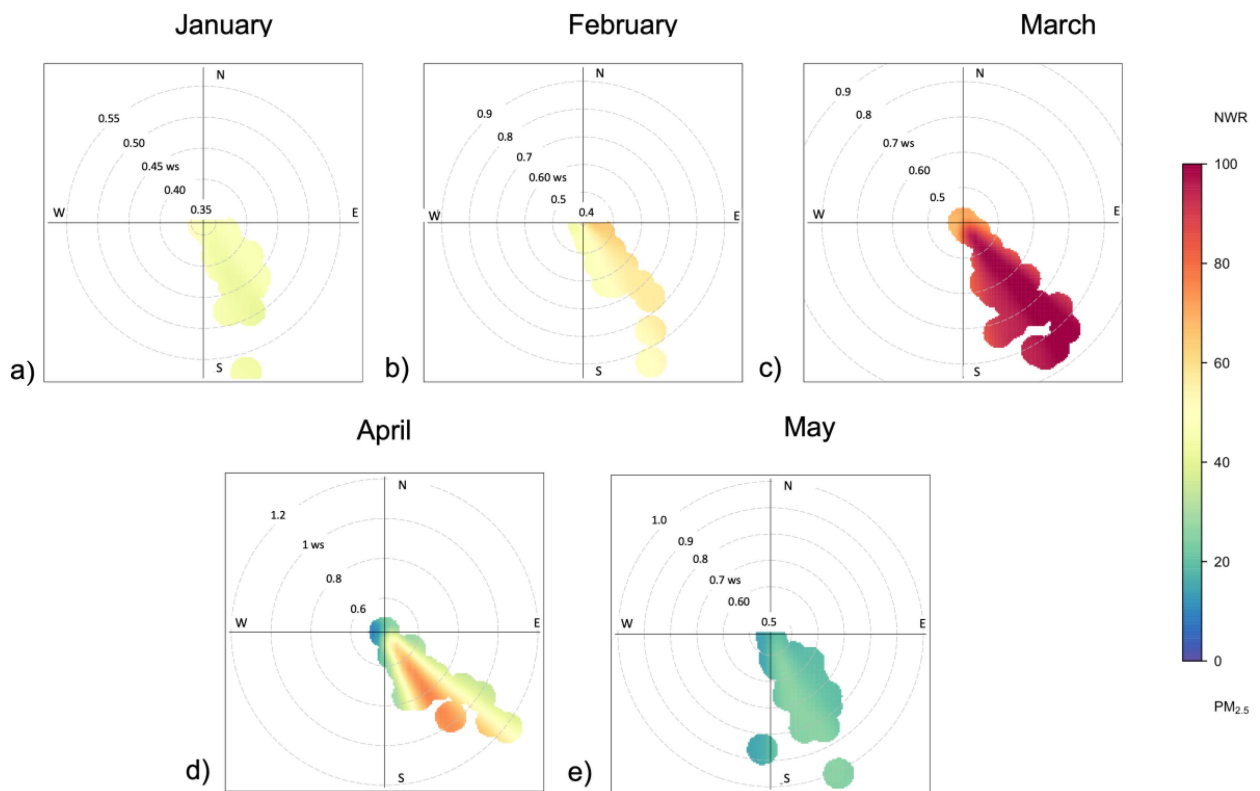


Figure 4. Polar plots of monthly concentrations of PM_{2.5} in (a) January, (b) February, (c) March, (d) April, and (e) May 2020 in northern Thailand.

The linear regression analysis between PM_{2.5} and meteorological variables is also shown in Figures 5–7. Figure 5 demonstrates a mainly negative relationship between wind speed and PM_{2.5} from January to May. These results are similar to previous studies, such as those by Wang and Ogawa [35], Ren et al. [36], and Sirithian et al. [37]. In general, the relative humidity and temperature were strongly correlated with the PM_{2.5} concentration; in contrast, the wind speed was slightly correlated with the PM_{2.5} concentration in northern Thailand. In cases where the wind speed is modest, pollutants could be blown away within a particular geographical area, but if the wind speed is strong, the huge amounts of pollutants could be transported from a long distance away. Between January and May, Figure 6 depicts the positive connection between temperature and PM_{2.5}. This result is similar to findings observed by Zhang et al. [38] and Han et al. [39]. Except for January, when a high negative correlation is observed, PM_{2.5} shows a mostly strong positive relationship with temperature during the rest of the months. This is due to the fact that temperature influences particle formation; hence, a high temperature increases the photochemical reaction between precursors, whilst a low temperature might delay the process and contribute to PM_{2.5}. The linear correlation between PM_{2.5} concentration and relative humidity is depicted in Figure 7. During most months, PM_{2.5} has a strong inverse relationship with relative humidity, similar to findings by Liu et al. [40]. Positive correlations were found in February, although the correlation coefficient is relatively low. When the humidity exceeds 70% in April and May, PM_{2.5} concentration shows a strong negative correlation with relative humidity. The Pearson correlation coefficient also highlights the relationships between PM_{2.5} and meteorological variables. There is a strong negative correlation between PM_{2.5} and relative humidity ranging between -0.88 and -0.49 and a weak correlation between PM_{2.5} and wind speed ranging between -0.096 and 0.087 , as well as a positive correlation related to temperature ranging between 0.56 and 0.70 . According to the findings, an increase in surface temperature and a reduction in relative humidity during the summer season had a significant impact on PM_{2.5} concentrations in northern Thailand.

In this study, there was a negative correlation between relative humidity and PM_{2.5}. In general, relative humidity regulates particle movement and therefore can induce particulate matter to sink to the surface. As a result, if relative humidity increases, PM_{2.5} tends to decrease [41,42]. Moreover, airborne particles condense and become dense enough for both dry and wet deposition when relative humidity reaches the threshold, leading to much lower PM_{2.5} concentrations [39]. There is also a strong positive correlation between temperature and PM_{2.5}. Since temperature affects particle production, a high temperature may enhance the photochemical reaction involving precursors [38]. The higher temperatures speed up photochemical reactions, which raise precursor levels of PM_{2.5} and other secondary pollutants as well as PM_{2.5} concentrations [43,44]. However, there was a negative correlation in January. This type of detrimental effect is mostly brought on by temperature-related air convections and losses of PM_{2.5}. In addition, the negative relationship is likely due to high temperatures, which facilitate the air's convection, which leads to the diluting and dispersal of PM_{2.5} [44]. Turbulence, which is caused by intense thermal activity at high temperatures, speeds up the distribution of PM_{2.5} [21,22]. In addition, because of the low surface temperature in the winter, warming might cause temperature inversion layers, which are unfavorable for airflow and may encourage the accumulation of PM_{2.5} [34]. The wind's direction also has a significant impact on PM_{2.5} concentrations. The wind carries various amounts of contaminants in various directions [45]. In general, when the wind is blowing at a moderate speed, contaminants can be dispersed within a small geographic area, but when the wind is strong enough, it can carry significant amounts of pollutants over considerable distances [45]. Furthermore, wind speed influences pollution levels in many different geographic regions [46]. For example, it has less of an impact on pollution levels in clean environments, such as forests, mountains, or coastal areas, while it increases pollution levels in megacities and heavily industrialized areas [46].

In this study, the relationship between wind speed and PM_{2.5} is inverse. This is most likely the outcome of several factors. The circumstances for PM_{2.5} diffusion are mostly made

perfect by an increase in wind speed, particularly a high wind speed [29]. Hence, increasing wind speed has a greater impact on removing PM_{2.5} concentrations from the atmosphere. Second, increased wind speed may result in larger evaporation losses and, thus, lower PM_{2.5} mass concentrations because wind speed is a key determinant in PM_{2.5} evaporation [30]. Wind speed may occasionally have a positive impact on PM_{2.5} concentrations. Initial increases in wind speed in light winds may result in low levels of turbulence, modest horizontal atmospheric movement, and a predominance of sinking movement in the upper air, creating unfavorable circumstances for PM_{2.5} and other pollutants to disperse [28,35].

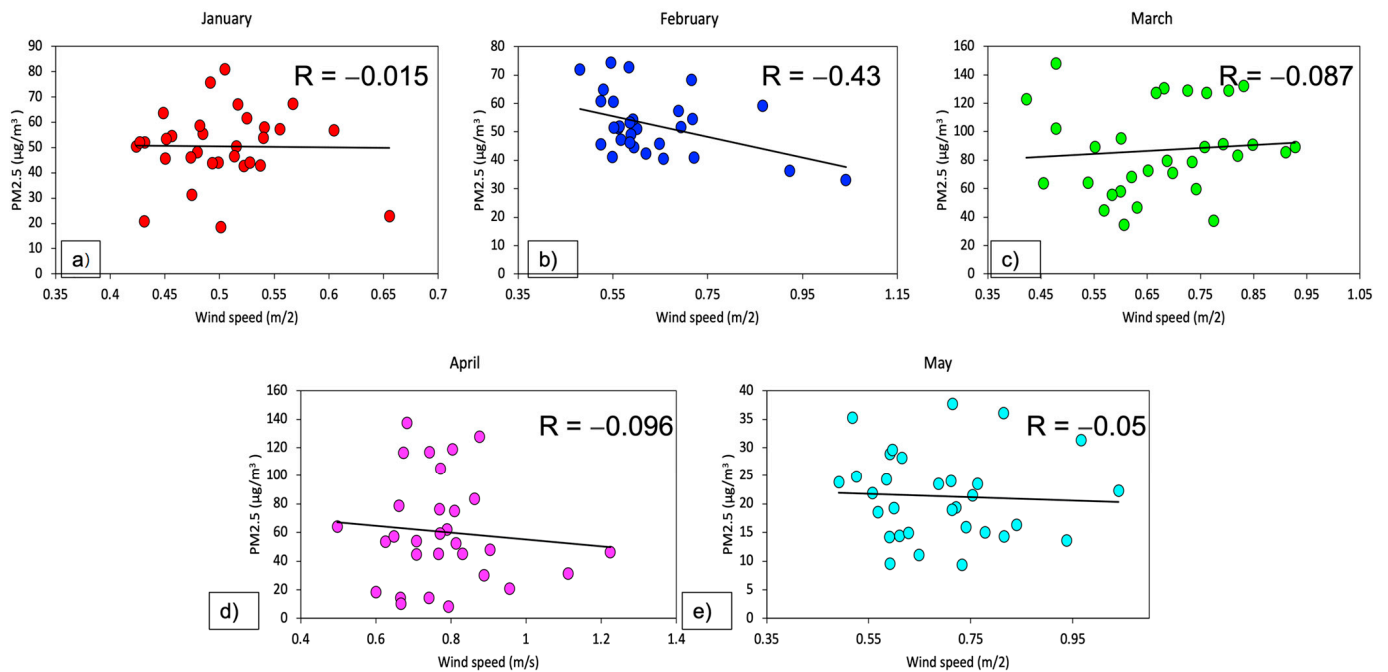


Figure 5. The association between PM_{2.5} and wind speed in (a) January, (b) February, (c) March, (d) April, and (e) May 2020.

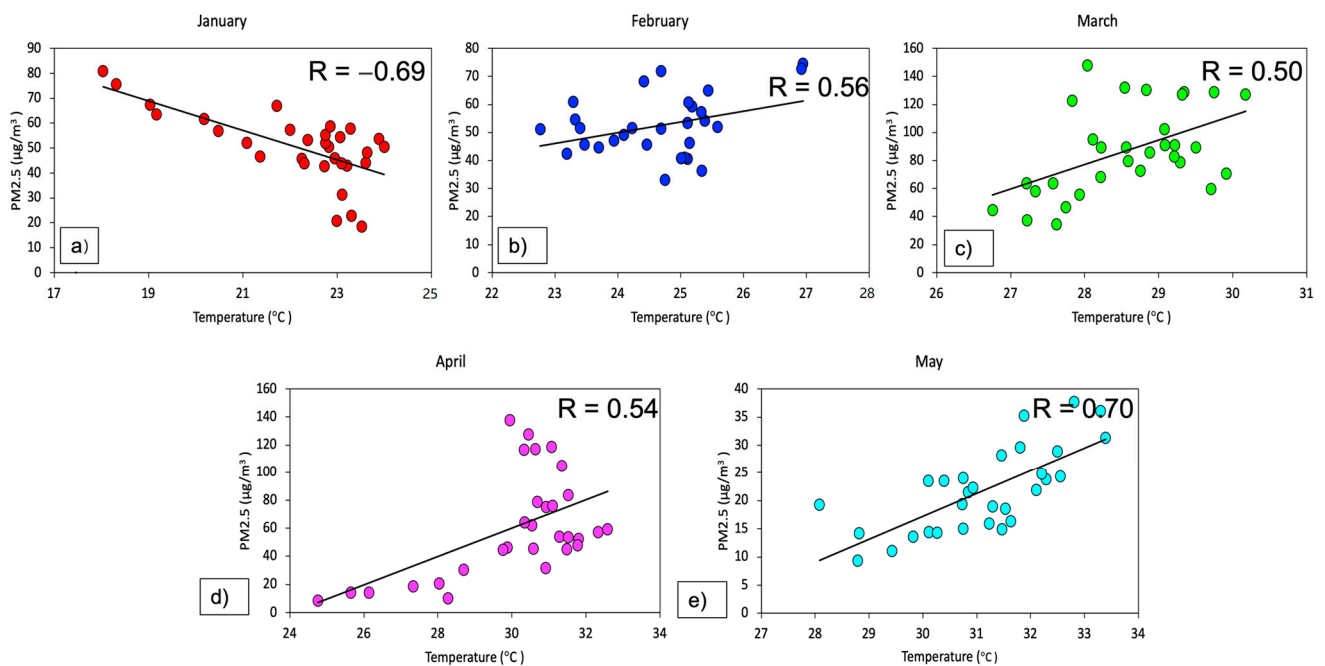


Figure 6. The association between PM_{2.5} and temperature in (a) January, (b) February, (c) March, (d) April, and (e) May 2020.

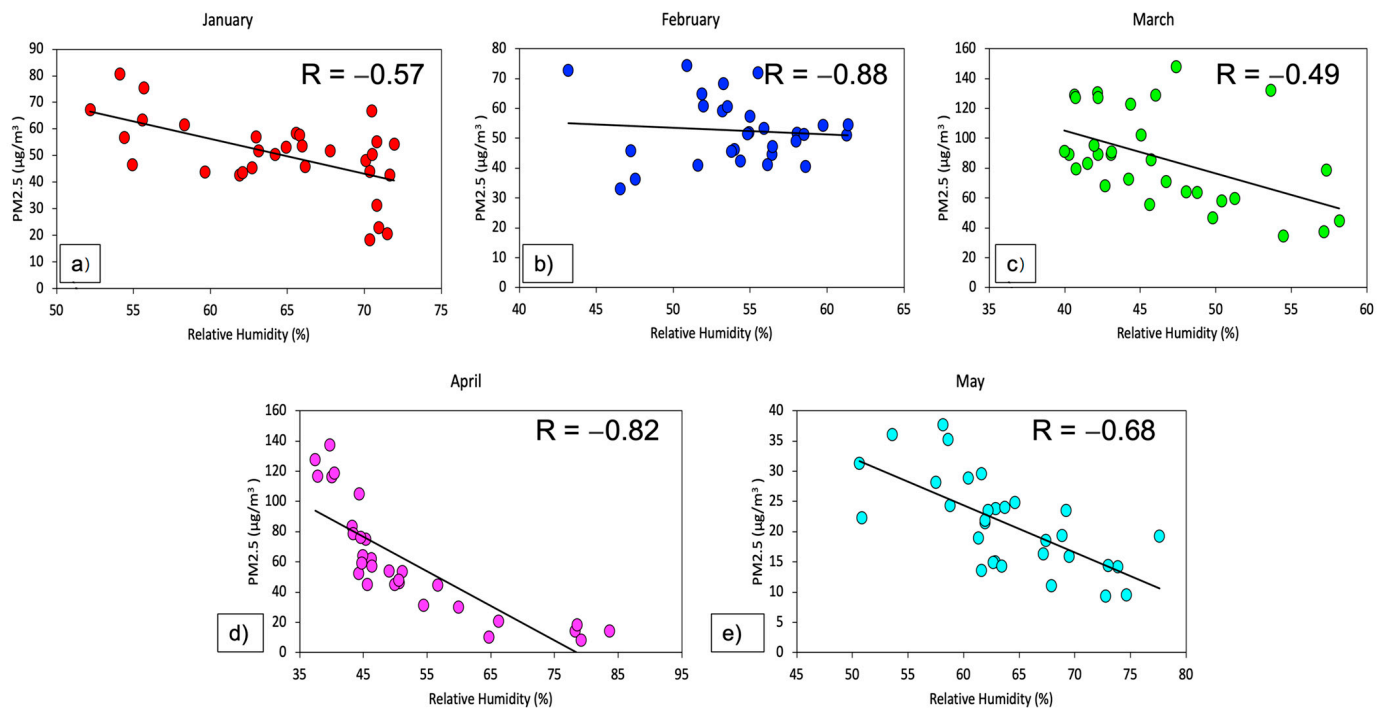


Figure 7. The relationship between $PM_{2.5}$ and humidity in (a) January, (b) February, (c) March, (d) April, and (e) May 2020.

3.3. $PM_{2.5}$, and Aerosol Optical Depth

Figures 8 and 9 show the spatial distribution of $PM_{2.5}$ (Figure 6) and aerosol optical depth (Figure 7). In general, the levels of $PM_{2.5}$ concentrations were in the range of 16 to $195 \mu\text{g}/\text{m}^3$ from January to May 2020. In January, the highest distribution of $PM_{2.5}$ concentrations was found in Lampang province, ranging from 150 to $195 \mu\text{g}/\text{m}^3$, while a range of 61 to $106 \mu\text{g}/\text{m}^3$ was found in the bulk of provinces. In February, the distribution of $PM_{2.5}$ concentrations in Chiang Rai province reached $195 \mu\text{g}/\text{m}^3$ at the top of the area. At the same time, $PM_{2.5}$ concentrations were in the range of 106 – $150 \mu\text{g}/\text{m}^3$ in the rest of northern Thailand. In March, the $PM_{2.5}$ concentrations were lower than in February, excluding the upper part of Chiang Rai province. In April, the $PM_{2.5}$ was more evenly distributed than it was in March in the entire region, with the concentration ranging from 106 to $195 \mu\text{g}/\text{m}^3$ in most of the region. In May, the $PM_{2.5}$ concentrations were similar to April, except the highest concentration was found in Chiang Mai province. The results of AOD from MERRA in Figure 4 correspond to the $PM_{2.5}$ concentration in Figure 3. AOD was generally in the range of 0.1 to 0.9 from January to April. In January, AOD was not too high for the whole region, while it tended to increase in February, reaching 0.6 in Lampang, Chiang Rai, and Phayao provinces. In March, AOD increased by 0.7 in many provinces, such as Chiang Rai, Phayao, Nan, and Phrae. In April, AOD was extremely high in most areas including Chiang Rai, Phayao, Nan, Phrae, Lampang, and Chiang Mai, ranging from 0.7 to 0.9.

There are numerous similarities between $PM_{2.5}$ and AOD, despite the fact that their association is not always reliable [47,48]. While AOD represents the entire atmospheric column, $PM_{2.5}$ primarily represents the atmospheric turbidity near the surface. Additionally, because $PM_{2.5}$ primarily represents the concentration of dry mass of fine particles, which is barely influenced by coarse particles and water vapor, the AOD also takes into account the influence of these two factors. According to this study, the AOD pattern in northern Thailand and the $PM_{2.5}$ concentration are most likely related. The similar pattern between $PM_{2.5}$ and AODs is most likely caused by the variations in aerosol type and properties in this region according to Yang et al. [49], who examined the relationships between $PM_{2.5}$ and AOD in 368 Chinese cities from February 2013 to December 2017 at various temporal

and regional scales. In their study, urban regions, which are similar to the study area in this paper, also showed a strong association between PM_{2.5} and AOD.

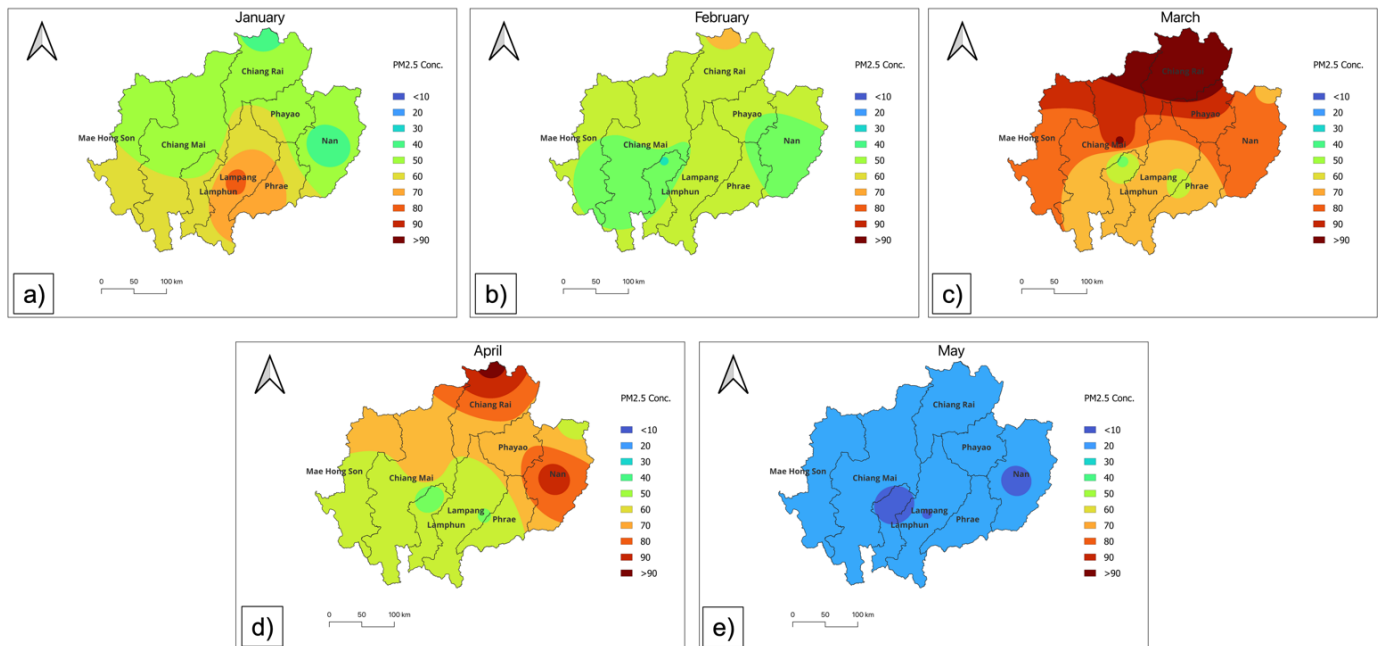


Figure 8. Spatial distribution of monthly averaged PM_{2.5} concentration ($\mu\text{g}/\text{m}^3$) in (a) January, (b) February, (c) March, (d) April, and (e) May in the year 2020.

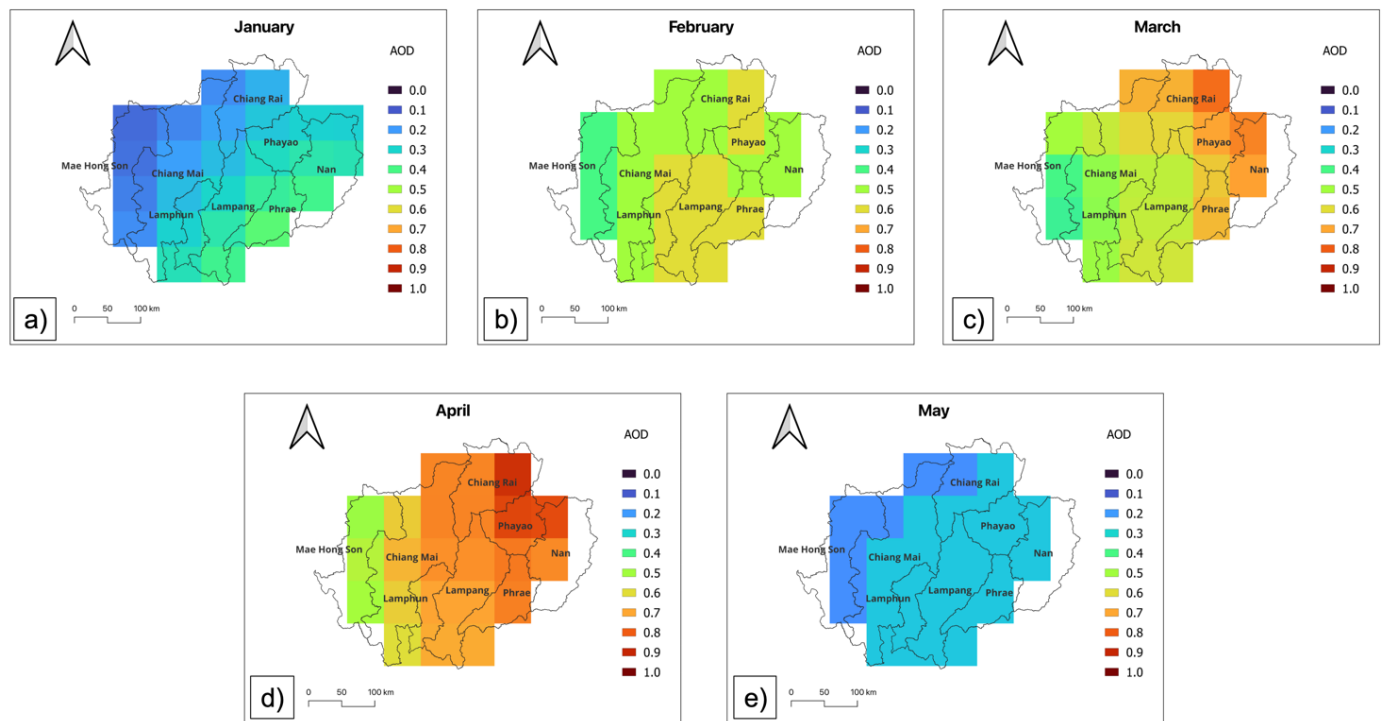


Figure 9. Spatial distribution of monthly averaged aerosol optical depth from MERRA in (a) January, (b) February, (c) March, (d) April, and (e) May in the year 2020.

3.4. Fire, Plume, and Visibility

The smoke plume and fire in the months of January, February, March, April, and May 2020 are shown in the images from NASA satellites taken by the Moderate Resolution

Integrated Aging Spectroradiometer (MODIS). The massive plumes of smoke were seen billowing across the majority of northern Thailand. No rain clouds are expected to arrive to put an end to the burning and smoke that are engulfing the area. Furthermore, from January to May, images of multiple fires growing in northern Thailand were captured by the NOAA/NASA Suomi NPP and NOAA 20 satellites (Figure 10). The area appears to be completely aflame (Figure 11). Agricultural burning is the most likely reason for the fires in this region [3]. It is likely due to the farmers burning their fields to prepare for the new planting season in Southeast Asia at this time of year.

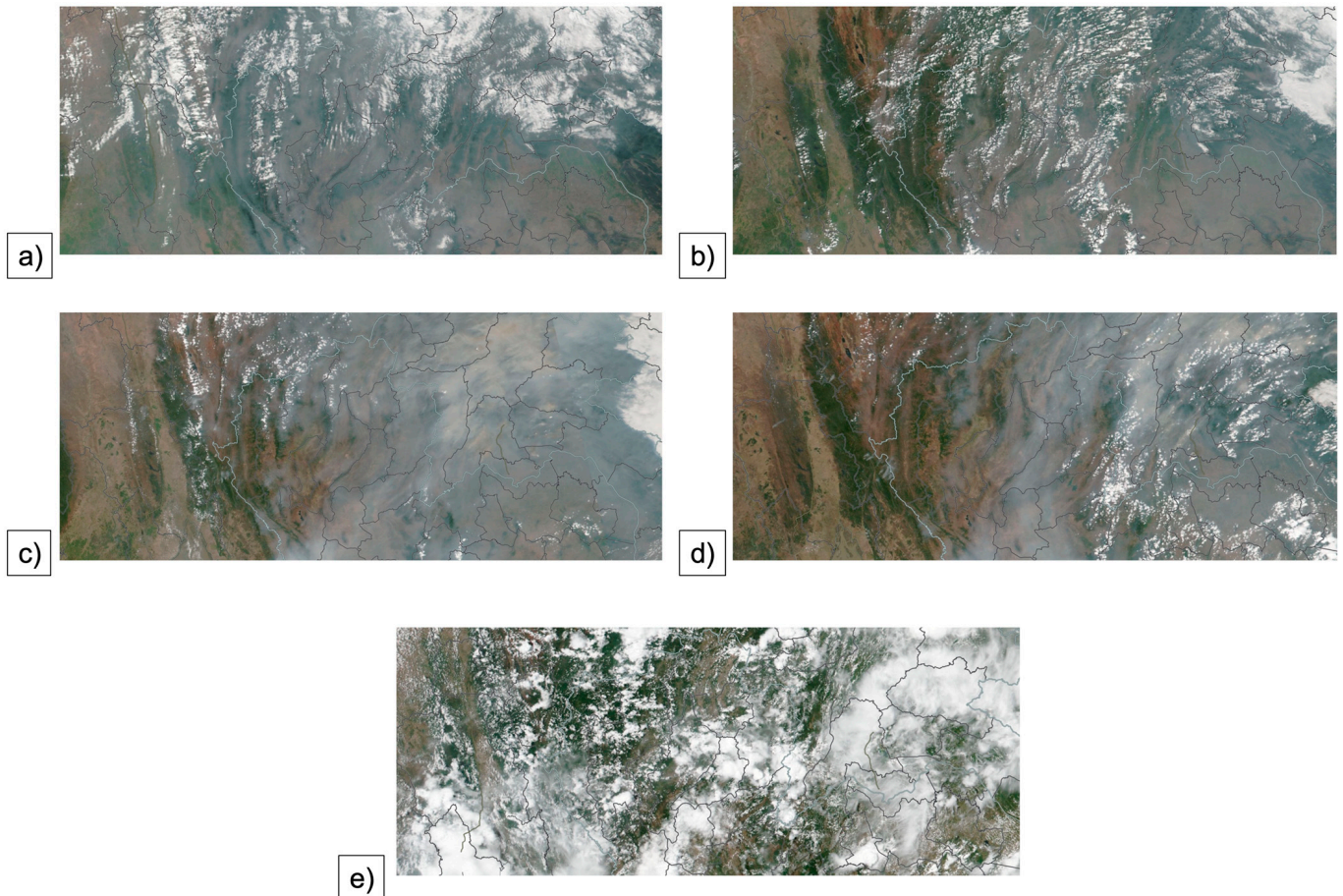


Figure 10. Satellite image from VIIR S-NPP corrected reflectance (true color) in (a) January, (b) February, (c) March, (d) April, and (e) May 2020 over northern Thailand.

Figures 12–14 show the spatial distribution of visibility in northern Thailand in 2020. At mixing height level at 1 km above ground level, low visibility generally occurred in March and April by <4 km at Chiang Rai province in March (Figure 12c), and in the range of 4–6 km in many areas of upper northern Thailand (Figure 12d) in April, while there was very clear visibility in May (Figure 12e). In January, the visibility was very clear, ranging between 13 and 18 km, while it was reduced to 6– < 4 km during February and April. In general, at the mixing height level of 1.5 km above ground level, the visibility is clearer than at 1.0 km, and the lowest visibility was also found in the range of 7–9 km in March and April in Chiang Rai province. The visibility was very clear in January and May with a value of 15–18 km; during February to April there was lower visibility. At the mixing height level of 3 km, the visibility was mostly clear compared to other levels ranging from 11–18 km for all months.

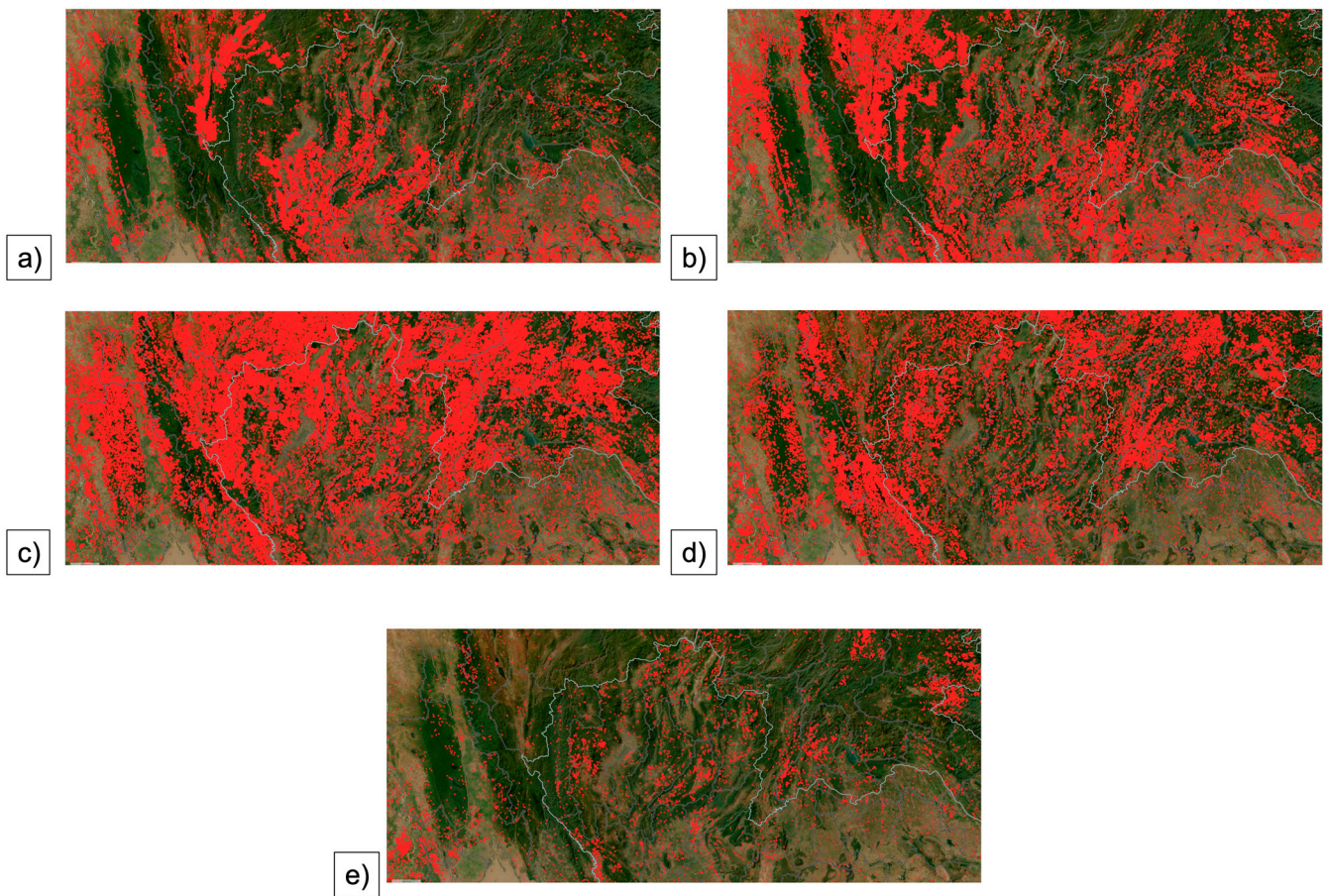


Figure 11. Satellite image from VIIRS (SUOMI NPP AND NOAA-20) in (a) January, (b) February, (c) March, (d) April, and (e) May 2020 over northern Thailand.

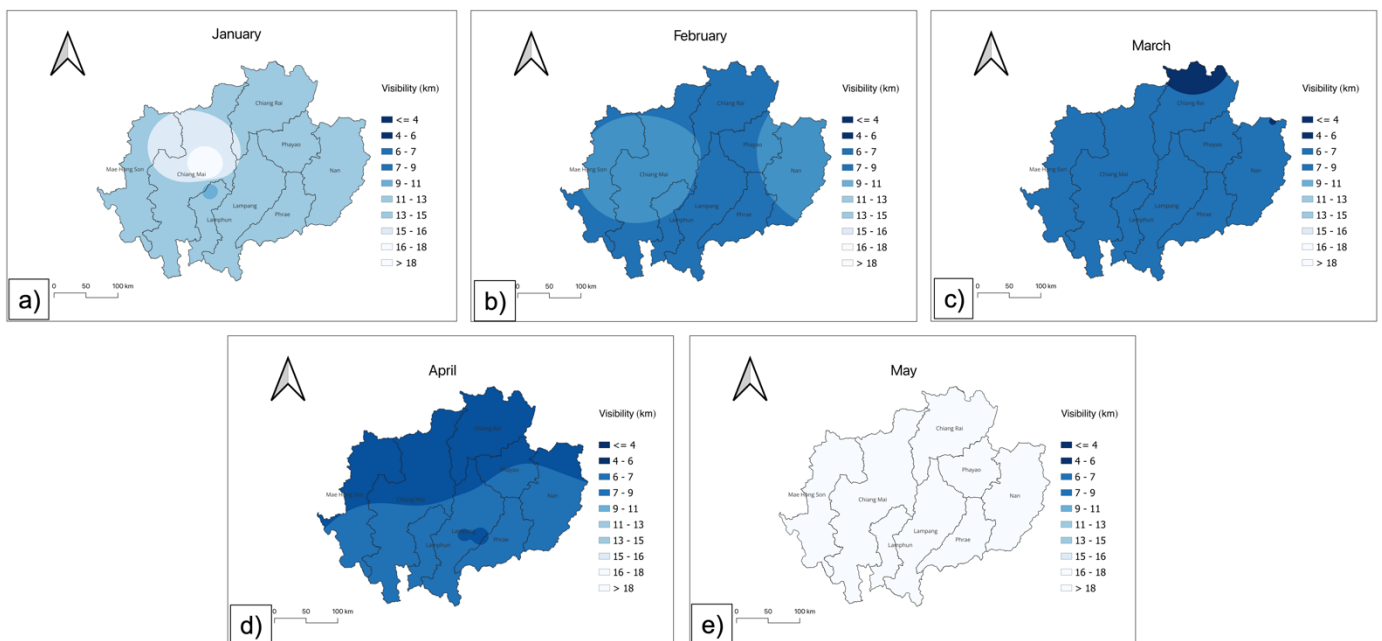


Figure 12. Spatial distribution of monthly averaged visibility at 1 km in (a) January, (b) February, (c) March, (d) April, and (e) May in the year 2020.

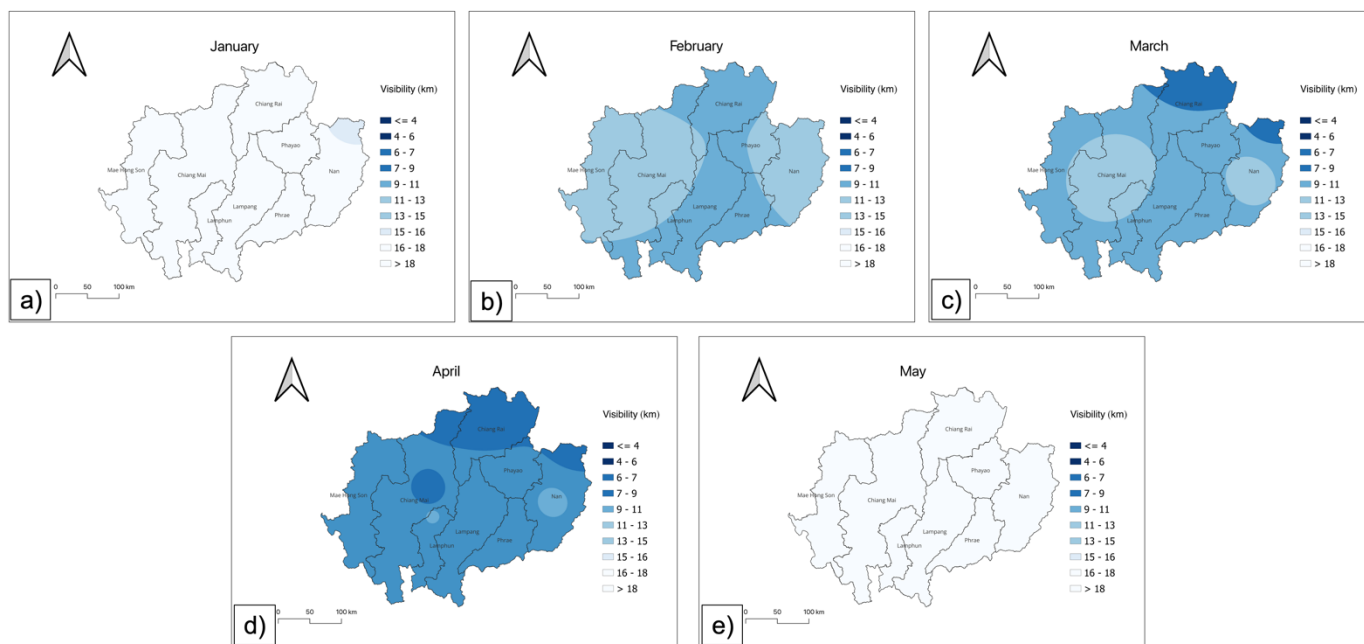


Figure 13. Spatial distribution of monthly averaged visibility at 1.5 km in (a) January, (b) February, (c) March, (d) April, and (e) May in the year 2020.

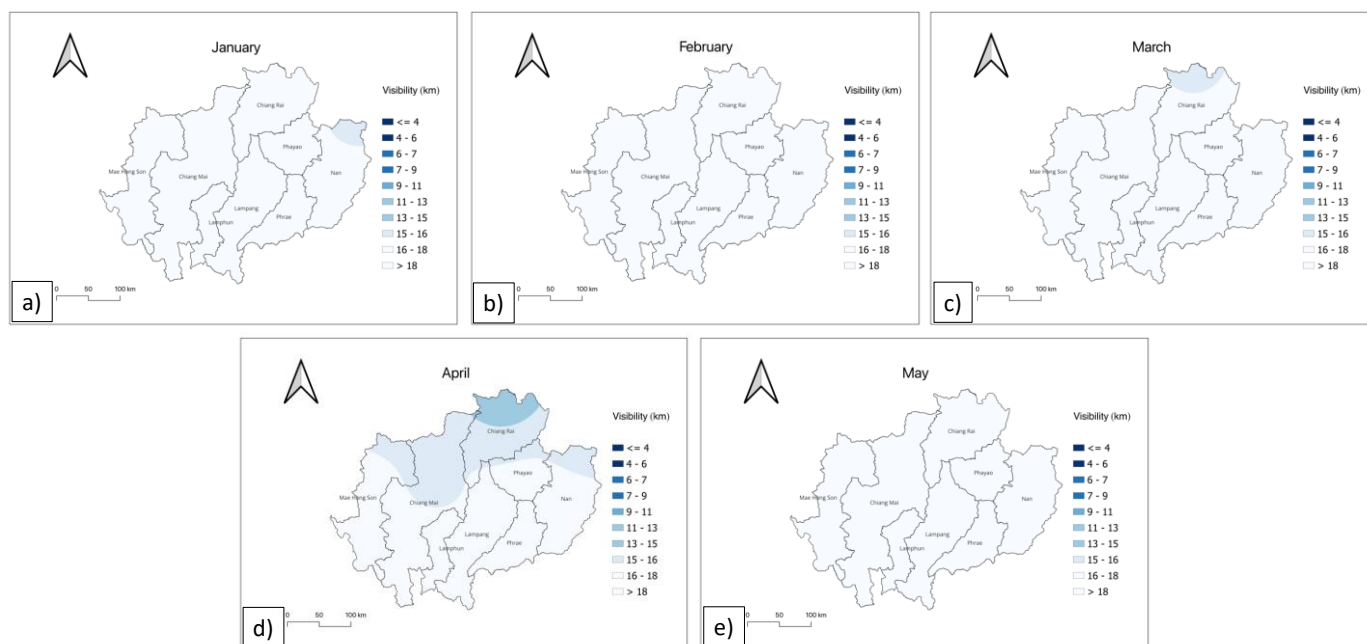


Figure 14. Spatial distribution of monthly averaged visibility at 3 km in (a) January, (b) February, (c) March, (d) April, and (e) May in the year 2020.

In comparison to the very clear visibility in May, during the haze months (January to April), PM_{2.5} tends to reduce visibility for all provinces (Figure 15). PM_{2.5} potentially reduces visibility in the range of 20–70%, 60–80%, 60–90%, and 70–90% in January, February, March, and April 2020 for all provinces. Massive fires in both domestic areas and areas surrounding northern Thailand from January to April contribute to huge amounts of smoke that cause low visibility in northern Thailand, especially at 1 km above ground level, with reduced visibility in the range of 70–90% for all provinces in April. As displayed in Table 2, during the haze episode (January to April), a 1 µg/m³ increase in PM_{2.5} essentially reduced visibility 0.30 ± 0.05, 0.83 ± 0.33, 0.32 ± 0.07, 0.48 ± 0.05, and 0.31 ± 0.04 in Chiang Mai,

Chiang Rai, Lamphun, Lamphun, and Nan provinces, respectively. At the same time, it was associated with a visibility reduction in range of 0.18–0.35 km, 0.20–1.74 km, 0.13–0.42 km, 0.34–0.56 km, and 0.23–0.42 km in Chiang Mai, Chiang Rai, Lamphun, Lamphun, and Nan provinces, respectively.

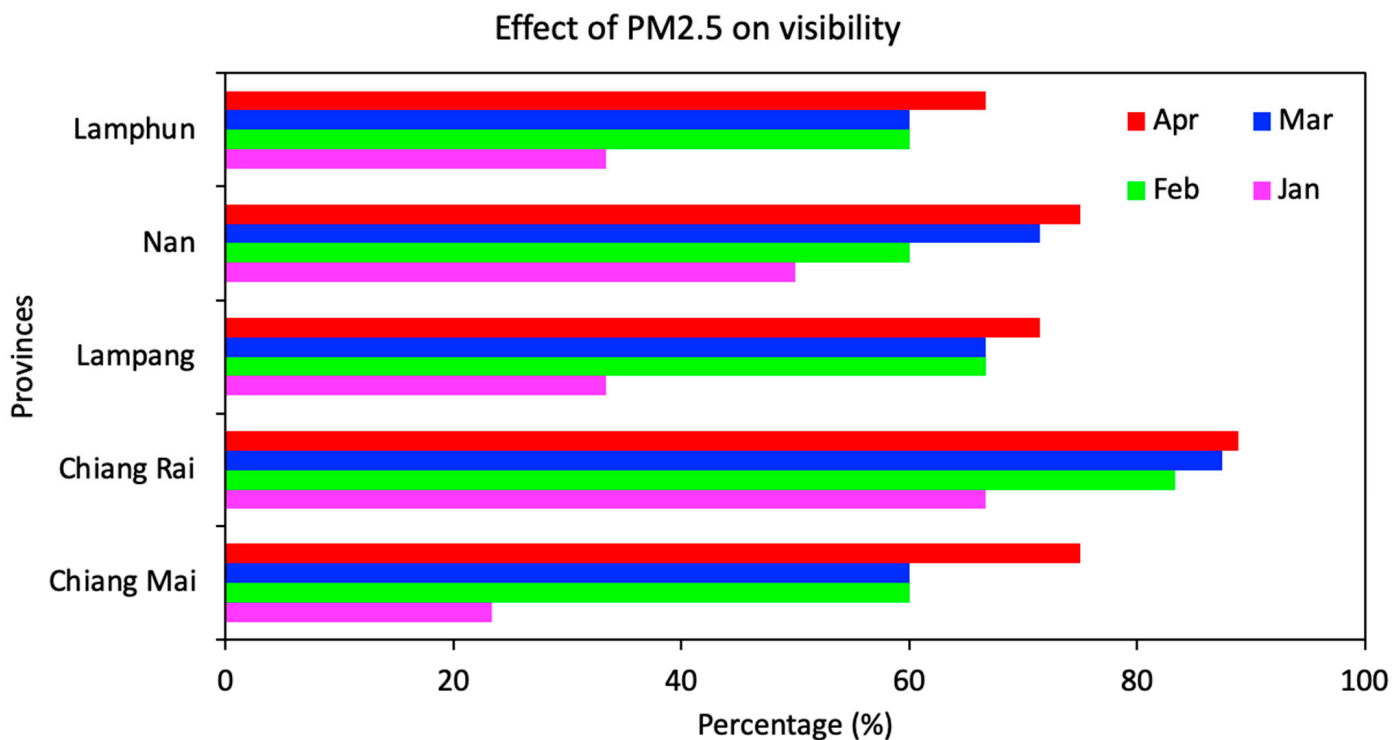


Figure 15. Percentage of difference in visibility in January (red), February (green), March (blue), and April (red) compared to background (May).

Table 2. Per 1 µg/m³ increase in PM_{2.5} was associated with a visibility at mixing height level of 1 km in five provinces of northern Thailand.

Month	Visibility (km)				
	Chiang Mai	Chiang Rai	Lampang	Lamphun	Nan
January	0.29	1.74	0.13	0.34	0.33
February	0.40	0.86	0.38	0.53	0.42
March	0.18	0.20	0.33	0.48	0.23
April	0.35	0.50	0.42	0.56	0.27
Mean	0.30 ± 0.05	0.83 ± 0.33	0.32 ± 0.07	0.48 ± 0.05	0.31 ± 0.04

The results of this demonstrate that the high level of PM_{2.5} is likely to be the primary cause of the reduction of visibility in northern Thailand, which is similar to findings by Zhao et al. [50] and Sloane et al. [51]. Although there are other elements that affect atmospheric visibility besides ambient air pollution, meteorological parameters, particularly humidity, have a substantial direct and indirect impact on visibility degradation [52]. However, fine particulate matter is the main pollutant in most urban areas [53,54], and its detrimental effects on visibility have drawn attention all over the world [55]. While the haze event in northern Thailand takes place during the dry season with very low relative humidity ranging from 30 to 60% (Figure 5b), PM_{2.5} is the primary reason for the area’s poor visibility.

3.5. Air Pollution Mitigation

It is evident that air pollution is a regional problem in Southeast Asia. Since air has no boundaries, only regional cooperation can address the issue of air pollution [56]. Although most countries in Southeast Asia (SEA) are aware of the difficulties caused by transboundary air pollution, no long-lasting solutions have been found [57]. Transboundary international environmental law is desperately needed to prevent the polluting countries from further deterioration. The ASEAN Agreement on Transboundary Haze Pollution (AATHP), a legally enforceable regional agreement, was established to tackle the haze issue in SEA [58]. The AATHP, however, is usually seen as a failure [59,60]. Reaching a regional agreement on the issue of atmospheric pollution has proven challenging due to uncertainties surrounding the identification of pollutant sources' locations [61,62].

Although there are several ways to identify transboundary air pollution, none are commonly used. Determining transboundary air pollution requires an understanding of the relationships between pollution emissions and the types, amounts, and consequences of depositions in receiving areas [63]. The issue of transboundary air pollution may be resolved by better knowledge of the scientific understanding of the source–receptor interaction in this region [64]. Insufficient in situ sampling and measurement of air pollutants, uncertainty in space-borne observation, and an inadequate emission inventory analysis (EIA) in the area are a few of the concerns that need to be addressed. The foundation of satellite remote sensing and numerical modeling approaches to determine transboundary air pollution is in situ sampling and measurements. The density and distribution of monitoring sites over SEA has not been adequate. Local administrations that run monitoring stations are present in just seven out of the ten ASEAN nations. In less economically developed nations, poor levels of maintenance at existing monitoring stations are another issue. Moreover, one of the primary causes of air pollution in the Indochina peninsula is biomass burning [65]. The three countries with the most fires in this region are Burma, Cambodia, and Laos, according to satellite-borne measurements [66]. The results of the contributions to transboundary air pollution from various geographic sources provide some information for policymaking.

Moreover, because fire from forests is a huge contributory source of smoke plume in SEA, forest fuel management is recommended for policymakers [67]. Prescribed burning is the best strategy for controlling forest fires in many nations. For example, during the dry season, a significant amount of leaf litter is produced by the forest, particularly in the north and west of Thailand. Specific parts may need to be incinerated for disposal, which must be performed at the proper time and location [67]. This will lessen smog brought on by out-of-control forest fires, preserve the health of the forest, and lessen damage from forest fires. Despite the fact that there are ongoing efforts to reduce, recycle, and utilize forest leftovers and large forest regions are always protected with fire barriers, it is challenging to maintain and govern huge forests. A zero-burning policy can reportedly reduce open burning activities in northern Thailand, according to Yabueng et al. [68]. Although biomass fires' fine particle levels have decreased, there are still extensive areas of smoke haze. The PM_{2.5} fraction reduced during the period when the policy for prohibiting open fires was extended from two months (middle of February through middle of April) to around three months (middle of February through middle of May). Hence, while the regulation is being implemented, open burning incidents can be decreased. According to the description above, particulate matter, which contributes to several air pollution issues, is often generated by biomass or lignocellulosic biomass waste. However, this substance might be turned into high-value goods, such as biomaterials, biochemicals, and fuels [69]. This process of valuing could also reduce the CO₂ and PM emissions brought on by the direct burning of a significant volume of biomass, which causes air pollution.

These initiatives are impossible to carry out without regional collaboration and the political will to push forward policies that aim to address poor air quality. Due to these considerations, tackling problems might be just as political or environmental. Governments in the area will need to make long-term financial and political commitments to pollution monitoring and research, as well as to sharing information and effectively responding to

evidence of chronically poor air quality, in order to meet this challenge. For administrators of the environment and decision makers in charge of making policies at the municipal, national, and regional levels, this study could potentially offer information that is essential. Without solid recommendations and counsel based on scientific knowledge and competence, decision making cannot be accomplished effectively. This is also true of diplomatic efforts to reduce air pollution in this region that are successful and efficient.

3.6. Limitation of the Study

Linear regression cannot adequately describe the relationship between $PM_{2.5}$ and meteorological variables because these interactions are rarely linear in real environments. For instance, various mechanisms explain how meteorological conditions influence the accumulation and dispersion of $PM_{2.5}$ [70]. Meteorological conditions and $PM_{2.5}$ levels both influence the complicated relationships between $PM_{2.5}$ and meteorology [71]. As a result, there are noticeable characteristics of meteorological influences on $PM_{2.5}$ concentrations due to considerable fluctuations in meteorological circumstances and $PM_{2.5}$ concentrations. For linearly separable data, however, linear regression performs remarkably well. Furthermore, it is simpler to use and understand and effective for explanation.

4. Conclusions

This study aims to investigate the distribution of $PM_{2.5}$ and how meteorological conditions control its accumulation, as well as the effect of $PM_{2.5}$ on visibility in northern Thailand in 2020. Several datasets were used in this study, including ground-based measurements from the Pollution Control Department in northern Thailand, aerosol optical depth (AOD) data from Modern-Era Retrospective Analysis for Research and Applications version 2 (MERRA-2), and satellite images from VIIRS S-NPP CORRECTED REFLECTANCE (TRUE COLOR) and VIIRS NOAA-20. The spatial distribution was utilized by GIS analysis. The daily average of $PM_{2.5}$ concentrations exceeded both Thailand's and the USEPA's standards, especially from January to May. The highest values of $PM_{2.5}$ concentrations were reported between 150 and 195 $\mu\text{g}/\text{m}^3$ from March to April. The favorable weather conditions induced the accumulation of $PM_{2.5}$ in northern Thailand. $PM_{2.5}$ had a negative association with both wind speed and relative humidity, although it had a positive correlation with temperature. The high $PM_{2.5}$ values in northern Thailand were caused by favorable climatic conditions. Because of the high concentration of $PM_{2.5}$, AOD ranged from 0.1 to 0.9 from January to April. AODs ranging from 0.7 to 0.9 have been recorded in Chiang Rai, Phayao, Nan, Phrae, Lampang, and Chiang Mai provinces, particularly in March and April. Between January and April, a massive fire from both domestic sources and neighboring countries contributed to huge plumes of smoke that were a long-range transport of pollutants to Thailand. As a result, visibility was reduced by up to 90% when compared to normal conditions.

Author Contributions: Conceptualization, T.A.; methodology, P.K., P.P. and T.A.; software, T.A.; validation, T.A.; formal analysis, T.A.; investigation, P.K., P.P. and T.A.; resources, T.A.; data curation, P.K., P.P. and T.A.; writing—original draft preparation, T.A.; writing—review and editing, T.A.; visualization, T.A.; supervision, T.A.; project administration, T.A.; funding acquisition, T.A. All authors have read and agreed to the published version of the manuscript.

Funding: This research was funded by University of Phayao and the APC was funded by University of Phayao.

Data Availability Statement: The data presented in this study are available in this article.

Acknowledgments: We would like to thank the Pollution Control Department from Thailand for supporting ground-based measurement data.

Conflicts of Interest: The authors declare no conflict of interest.

References

1. Chen, J.; Li, Z.; Lv, M.; Wang, Y.; Wang, W.; Zhang, Y.; Wang, H.; Yan, X.; Sun, Y.; Cribb, M. Aerosol hygroscopic growth, contributing factors, and impact on haze events in a severely polluted region in northern China. *Atmos. Chem. Phys.* **2019**, *19*, 1327–1342. [[CrossRef](#)]
2. Wang, X.; Fu, T.M.; Zhang, L.; Lu, X.; Liu, X.; Amnuaylojaroen, T.; Latif, M.T.; Ma, Y.; Zhang, L.; Feng, X.; et al. Rapidly changing emissions drove substantial surface and tropospheric ozone increases over Southeast Asia. *Geo. Res. Lett.* **2022**, *49*, e2022GL100223. [[CrossRef](#)]
3. Amnuaylojaroen, T.; Inkom, J.; Janta, R.; Surapipith, V. Long range transport of southeast asian PM_{2.5} pollution to northern Thailand during high biomass burning episodes. *Sustainability* **2020**, *12*, 10049. [[CrossRef](#)]
4. Huang, W.-R.; Wang, S.-H.; Yen, M.-C.; Lin, N.-H.; Promchote, P. Interannual variation of springtime biomass burning in Indochina: Regional differences, associated atmospheric dynamical changes, and downwind impacts. *J. Geophys. Res. Atmos.* **2016**, *121*, 10016–10028. [[CrossRef](#)] [[PubMed](#)]
5. Yin, S.; Wang, X.; Zhang, X.; Guo, M.; Miura, M.; Xiao, Y. Influence of biomass burning on local air pollution in mainland Southeast Asia from 2001 to 2016. *Environ. Pollut.* **2019**, *254*, 112949. [[CrossRef](#)]
6. Amnuaylojaroen, T.; Barth, M.; Emmons, L.; Carmichael, G.; Kreasuwun, J.; Prasitwattanaseree, S.; Chantara, S. Effect of different emission inventories on modeled ozone and carbon monoxide in Southeast Asia. *Atmos. Chem. Phys.* **2014**, *14*, 12983–13012. [[CrossRef](#)]
7. Lee, H.-H.; Iraqui, O.; Gu, Y.; Yim, S.H.-L.; Chulakadabba, A.; Tonks, A.Y.-M.; Yang, Z.; Wang, C. Impacts of air pollutants from fire and non-fire emissions on the regional air quality in Southeast Asia. *Atmos. Chem. Phys.* **2018**, *18*, 6141–6156. [[CrossRef](#)]
8. Amnuaylojaroen, T.; Kreasuwun, J. Investigation of fine and coarse particulate matter from burning areas in Chiang Mai, Thailand using the WRF/CALPUFF. *Chiang Mai J. Sci.* **2012**, *39*, 311–326.
9. Khodmanee, S.; Amnuaylojaroen, T. Impact of Biomass Burning on Ozone, Carbon Monoxide, and Nitrogen Dioxide in Northern Thailand. *Front. Environ. Sci.* **2021**, *9*, 27. [[CrossRef](#)]
10. He, H.; Tie, X.; Zhang, Q.; Liu, X.; Gao, Q.; Li, X.; Gao, Y. Analysis of the causes of heavy aerosol pollution in Beijing, China: A case study with the WRF-Chem model. *Particuology* **2015**, *20*, 32–40. [[CrossRef](#)]
11. Pohjola, M.A.; Kousa, A.; Kukkonen, J.; Härkönen, J.; Karppinen, A.; Aarnio, P.; Koskentalo, T. The spatial and temporal variation of measured urban PM₁₀ and PM_{2.5} in the Helsinki metropolitan area. *Water Air Soil Pollut. Focus* **2002**, *2*, 189–201. [[CrossRef](#)]
12. Tai, A.P.; Mickley, L.J.; Jacob, D.J. Correlations between fine particulate matter (PM_{2.5}) and meteorological variables in the United States: Implications for the sensitivity of PM_{2.5} to climate change. *Atmos. Environ.* **2010**, *44*, 3976–3984. [[CrossRef](#)]
13. Akbal, Y.; Ünlü, K.D. A deep learning approach to model daily particular matter of Ankara: Key features and forecasting. *Int. J. Environ. Sci. Technol.* **2021**, *19*, 5911–5927. [[CrossRef](#)]
14. Shahriar, S.A.; Kayes, I.; Hasan, K.; Salam, M.A.; Chowdhury, S. Applicability of machine learning in modeling of atmospheric particle pollution in Bangladesh. *Air Qual. Atmos. Health* **2020**, *13*, 1247–1256. [[CrossRef](#)] [[PubMed](#)]
15. Franceschi, F.; Cobo, M.; Figueredo, M. Discovering relationships and forecasting PM₁₀ and PM_{2.5} concentrations in Bogotá, Colombia, using artificial neural networks, principal component analysis, and k-means clustering. *Atmos. Pollut. Res.* **2018**, *9*, 912–922. [[CrossRef](#)]
16. Feng, X.; Li, Q.; Zhu, Y.; Hou, J.; Jin, L.; Wang, J. Artificial neural networks forecasting of PM_{2.5} pollution using air mass trajectory based geographic model and wavelet transformation. *Atmos. Environ.* **2015**, *107*, 118–128. [[CrossRef](#)]
17. Akdi, Y.; Okkaoglu, Y.; Gölveren, E.; Yücel, M.E. Estimation and forecasting of PM 10 air pollution in Ankara via time series and harmonic regressions. *Int. J. Environ. Sci. Technol.* **2020**, *17*, 3677–3690. [[CrossRef](#)]
18. Zhao, J.; Kong, X.; He, K.; Xu, H.; Mu, J. Assessment of the radiation effect of aerosols on maize production in China. *Sci. Total Environ.* **2020**, *720*, 137567. [[CrossRef](#)]
19. Wei, K.; Tang, X.; Tang, G.; Wang, J.; Xu, L.; Li, J.; Ni, C.; Zhou, Y.; Ding, Y.; Liu, W. Distinction of two kinds of haze. *Atmos. Environ.* **2020**, *223*, 117228. [[CrossRef](#)]
20. Zeng, W.; Liu, T.; Du, Q.; Li, J.; Xiao, J.; Guo, L.; Li, X.; Xu, Y.; Xu, X.; Wan, D.; et al. The interplay of haze characteristics on mortality in the Pearl River Delta of China. *Environ. Res.* **2020**, *184*, 109279. [[CrossRef](#)]
21. Yang, X.; Zhao, C.; Guo, J.; Wang, Y. Intensification of aerosol pollution associated with its feedback with surface solar radiation and winds in Beijing. *J. Geophys. Res. Atmos.* **2016**, *121*, 4093–4099. [[CrossRef](#)]
22. Yang, X.; Zhao, C.; Zhou, L.; Wang, Y.; Liu, X. Distinct impact of different types of aerosols on surface solar radiation in China. *J. Geophys. Res. Atmos.* **2016**, *121*, 6459–6471. [[CrossRef](#)]
23. Zhang, X.; Zhang, Q.; Hong, C.; Zheng, Y.; Geng, G.; Tong, D.; Zhang, Y.; Zhang, X. Enhancement of PM_{2.5} concentrations by aerosol-meteorology interactions over China. *J. Geophys. Res. Atmos.* **2018**, *123*, 1179–1194. [[CrossRef](#)]
24. Liu, F.; Fang, P.; Yao, Z.; Fan, R.; Pan, Z.; Sheng, W.; Yang, H. Recovering 6D object pose from RGB indoor image based on two-stage detection network with multi-task loss. *Neurocomputing* **2019**, *337*, 15–23. [[CrossRef](#)]
25. Guan, L.; Liang, Y.; Tian, Y.; Yang, Z.; Sun, Y.; Feng, Y. Quantitatively analyzing effects of meteorology and PM_{2.5} sources on low visual distance. *Sci. Total Environ.* **2019**, *659*, 764–772. [[CrossRef](#)] [[PubMed](#)]
26. Wong, C.-M.; Vichit-Vadakan, N.; Kan, H.; Qian, Z. Public Health and Air Pollution in Asia (PAPA): A multicity study of short-term effects of air pollution on mortality. *Environ. Health Perspect.* **2008**, *116*, 1195–1202. [[CrossRef](#)] [[PubMed](#)]

27. Amnuaylojaroen, T. Prediction of PM_{2.5} in an urban area of northern Thailand using multivariate linear regression model. *Adv. Meteorol.* **2022**, *2022*, 3190484. [[CrossRef](#)]
28. Bedient, P.B.; Huber, W.C.; Vieux, B.E. *Hydrology and Floodplain Analysis*; Prentice Hall: Upper Saddle River, NJ, USA, 2008; Volume 816.
29. Burrough, P.A.; McDonnell, R.A.; Lloyd, C.D. *Principles of Geographical Information Systems*; Oxford University Press: Oxford, UK, 2015.
30. Bäumer, D.; Vogel, B.; Versick, S.; Rinke, R.; Möhler, O.; Schnaiter, M. Relationship of visibility, aerosol optical thickness and aerosol size distribution in an ageing air mass over South-West Germany. *Atmos. Environ.* **2008**, *42*, 989–998. [[CrossRef](#)]
31. Carabali, G.; Villanueva-Macias, J.; Ladino, L.A.; Álvarez-Ospina, H.; Raga, G.B.; Andraca-Ayala, G.; Miranda, J.; Grutter, M.; Silva, M.M.; Riveros-Rosas, D. Characterization of aerosol particles during a high pollution episode over Mexico City. *Sci. Rep.* **2021**, *11*, 22533. [[CrossRef](#)]
32. Amnuaylojaroen, T.; Macatangay, R.C.; Khodmanee, S. Modeling the effect of VOCs from biomass burning emissions on ozone pollution in upper Southeast Asia. *Heliyon* **2019**, *5*, e02661. [[CrossRef](#)]
33. Hama, S.M.; Kumar, P.; Harrison, R.M.; Bloss, W.J.; Khare, M.; Mishra, S.; Namdeo, A.; Sokhi, R.; Goodman, P.; Sharma, C. Four-year assessment of ambient particulate matter and trace gases in the Delhi-NCR region of India. *Sustain. Cities Soc.* **2020**, *54*, 102003. [[CrossRef](#)]
34. Shelton, S.; Liyanage, G.; Jayasekara, S.; Pushpawela, B.; Rathnayake, U.; Jayasundara, A.; Jayasooriya, L.D. Seasonal Variability of Air Pollutants and Their Relationships to Meteorological Parameters in an Urban Environment. *Adv. Meteorol.* **2022**, *2022*, 5628911. [[CrossRef](#)]
35. Wang, J.; Ogawa, S. Effects of meteorological conditions on PM_{2.5} concentrations in Nagasaki, Japan. *Int. J. Environ. Res. Public Health* **2015**, *12*, 9089–9101. [[CrossRef](#)] [[PubMed](#)]
36. Ren, J.; Liu, J.; Li, F.; Cao, X.; Ren, S.; Xu, B.; Zhu, Y. A study of ambient fine particles at Tianjin International Airport, China. *Sci. Total Environ.* **2016**, *556*, 126–135. [[CrossRef](#)]
37. Sirithian, D.; Thanatrakolsri, P. Relationships between Meteorological and Particulate Matter Concentrations (PM_{2.5} and PM₁₀) during the Haze Period in Urban and Rural Areas, Northern Thailand. *Air Soil Water Res.* **2022**, *15*, 1–15. [[CrossRef](#)]
38. Zhang, Z.; Gong, D.; Mao, R.; Kim, S.-J.; Xu, J.; Zhao, X.; Ma, Z. Cause and predictability for the severe haze pollution in downtown Beijing in November–December 2015. *Sci. Total Environ.* **2017**, *592*, 627–638. [[CrossRef](#)]
39. Han, J.; Wang, J.; Zhao, Y.; Wang, Q.; Zhang, B.; Li, H.; Zhai, J. Spatio-temporal variation of potential evapotranspiration and climatic drivers in the Jing-Jin-Ji region, North China. *Agric. For. Meteorol.* **2018**, *256*, 75–83. [[CrossRef](#)]
40. Liu, P.F.; Zhao, C.S.; Gbel, T.; Hallbauer, E.; Nowak, A.; Ran, L.; Xu, W.Y.; Deng, Z.Z.; Ma, N.; Mildemberger, K.; et al. Hygroscopic properties of aerosol particles at high relative humidity and their diurnal variations in the north china plain. *Atmos. Chem. Phys.* **2011**, *11*, 3479–3794. [[CrossRef](#)]
41. Giri, D.; Adhikary, P.R.; Murthy, V.K. The influence of meteorological conditions on PM₁₀ concentrations in Kathmandu Valley. *Int. J. Environ. Res.* **2008**, *2*, 49–60.
42. Kayes, I.; Shahriar, S.A.; Hasan, K.; Akhter, M.; Kabir, M.M.; Salam, M.A. The relationships between meteorological parameters and air pollutants in an urban environment. *Glob. J. Environ. Sci. Manag.* **2019**, *5*, 265–278. [[CrossRef](#)]
43. Luo, J.; Du, P.; Samat, A.; Xia, J.; Che, M.; Xue, Z. Spatiotemporal Pattern of PM_{2.5} Concentrations in Mainland China and Analysis of Its Influencing Factors using Geographically Weighted Regression. *Sci. Rep.* **2017**, *7*, 40607. [[CrossRef](#)] [[PubMed](#)]
44. Zhang, C.; Ni, Z.; Ni, L. Multifractal detrended cross-correlation analysis between PM_{2.5} and meteorological factors. *Phys. A Stat. Mech. Its Appl.* **2015**, *438*, 114–123. [[CrossRef](#)]
45. Wang, M.; Cao, C.; Li, G.; Singh, R.P. Analysis of a severe prolonged regional haze episode in the Yangtze River Delta, China. *Atmos. Environ.* **2015**, *102*, 112–121. [[CrossRef](#)]
46. Pushpawela, B.; Jayaratne, R.; Morawska, L. The influence of wind speed on new particle formation events in an urban environment. *Atmos. Res.* **2019**, *1*, 37–41. [[CrossRef](#)]
47. Zhang, Y.; Li, Z. Remote sensing of atmospheric fine particulate matter (PM_{2.5}) mass concentration near the ground from satellite observation. *Remote Sens. Environ.* **2015**, *160*, 252–262. [[CrossRef](#)]
48. Zheng, C.; Zhao, C.; Zhu, Y.; Wang, Y.; Shi, X.; Wu, X.; Chen, T.; Wu, F.; Qiu, Y. Analysis of influential factors for the relationship between PM_{2.5} and AOD in Beijing. *Atmos. Chem. Phys.* **2017**, *17*, 13473–13489. [[CrossRef](#)]
49. Yang, Q.; Yuan, Q.; Li, T.; Shen, H.; Zhang, L. The relationships between PM_{2.5} and meteorological factors in China: Seasonal and regional variations. *Int. J. Environ. Res. Public Health* **2017**, *14*, 1510. [[CrossRef](#)]
50. Zhao, X.J.; Zhang, X.L.; Xu, X.F.; Xu, J.; Meng, W.; Pu, W.W. Seasonal and diurnal variations of ambient PM_{2.5} concentration in urban and rural environments in Beijing. *Atmos. Environ.* **2009**, *43*, 2893–2900. [[CrossRef](#)]
51. Sloane, C.S.; Watson, J.; Chow, J.; Pritchett, L.; Willard Richards, L. Size-segregated fine particle measurements by chemical species and their impact on visibility impairment in Denver. *Atmos. Environ. Part A Gen. Top.* **1991**, *25*, 1013–1024. [[CrossRef](#)]
52. Yang, Z.; Wang, Y.; Xu, X.H.; Yang, J.; Ou, C.Q. Quantifying and characterizing the impacts of PM_{2.5} and humidity on atmospheric visibility in 182 Chinese cities: A nationwide time-series study. *J. Clean. Prod.* **2022**, *368*, 133182. [[CrossRef](#)]
53. Zhang, H.; Hoff, R.M.; Engel-Cox, J.A. The relation between Moderate Resolution Imaging Spectroradiometer (MODIS) aerosol optical depth and PM_{2.5} over the United States: A geographical comparison by US Environmental Protection Agency regions. *J. Air Waste Manag. Assoc.* **2009**, *59*, 1358–1369. [[CrossRef](#)] [[PubMed](#)]

54. Zhang, Q.; Streets, D.G.; Carmichael, G.R.; He, K.B.; Huo, H.; Kannari, A.; Klimont, Z.; Park, I.S.; Reddy, S.; Fu, J.S.; et al. Asian emissions in 2006 for the NASA INTEX–B mission. *Atmos. Chem. Phys.* **2009**, *9*, 5131–5153. [[CrossRef](#)]
55. Aouizerats, B.; Van Der Werf, G.R.; Balasubramanian, R.; Betha, R. Importance of transboundary transport of biomass burning emissions to regional air quality in Southeast Asia during a high fire event. *Atmos. Chem. Phys.* **2015**, *15*, 363–373. [[CrossRef](#)]
56. Jones, D.S. ASEAN and transboundary haze pollution in Southeast Asia. *Asia Eur. J.* **2006**, *4*, 431–446. [[CrossRef](#)]
57. ASEAN Cooperation on Environment. Indonesia Deposits Instrument of Ratification of the ASEAN Agreement on Transboundary Haze Pollution. 2015. Available online: <https://environment.asean.org/indonesia-deposits-instrument-of-ratification-of-the-asean-agreement-on-transboundary-haze-pollution/> (accessed on 9 March 2023).
58. Forsyth, T. Public concerns about transboundary haze: A comparison of Indonesia, Singapore, and Malaysia. *Global Environ. Chang.* **2014**, *25*, 76–86. [[CrossRef](#)]
59. Nurhidayah, L.; Lipman, Z.; Alam, S. Regional environmental governance: An evaluation of the ASEAN legal framework for addressing transboundary haze pollution. *Aust. J. Asian Law* **2014**, *15*, 87.
60. Hook, G.D.; Mason, R.; O’Shea, P. *Regional Risk and Security in Japan: Whither the Everyday*; Taylor & Francis: Abingdon, UK, 2015.
61. Nobuhiko, S. We Cannot Afford to See PM_{2.5} Pollution Indifferently. Global Forum of Japan Commentary. Available online: <http://www.gfj.jp/e/commentary/130426.pdf> (accessed on 6 March 2023).
62. Venkatram, A.; Karamchandani, P. Source-receptor relationships. A look at acid deposition modeling. *Environ. Sci. Technol.* **1986**, *20*, 1084–1091. [[CrossRef](#)]
63. Chen, Q.; Taylor, D. Transboundary atmospheric pollution in Southeast Asia: Current methods, limitations and future developments. *Crit. Rev. Environ. Sci. Technol.* **2018**, *48*, 997. [[CrossRef](#)]
64. Yadav, I.C.; Devi, N.L.; Li, J.; Syed, J.H.; Zhang, G.; Watanabe, H. Biomass burning in Indo-China peninsula and its impacts on regional air quality and global climate change: A review. *Environ. Pollut.* **2017**, *227*, 414–427. [[CrossRef](#)]
65. Vadrevu, K.P.; Justice, C. Vegetation fires in the Asian region: Satellite observational needs and priorities. *Global Environ. Res.* **2011**, *15*, 65–76.
66. Suriyawong, P.; Chuetor, S.; Samae, H.; Piriyaakarnsakul, S.; Amin, M.; Furuuchi, M.; Hata, M.; Inerb, M.; Phairuang, W. Airborne particulate matter from biomass burning in Thailand: Recent issues, challenges, and options. *Heliyon* **2023**, *9*, e14261. [[CrossRef](#)]
67. Chernkhunthod, C.; Hioki, Y. Fuel characteristics and fire behavior in mixed deciduous forest areas with different fire frequencies in Doi Suthep-Pui National Park, Northern Thailand. *Landsc. Ecol. Eng.* **2020**, *16*, 289–297. [[CrossRef](#)]
68. Yabueng, N.; Wiriya, W.; Chantara, S. Influence of zero-burning policy and climate phenomena on ambient PM_{2.5} patterns and PAHs inhalation cancer risk during episodes of smoke haze in Northern Thailand. *Atmos. Environ.* **2020**, *232*, 117485. [[CrossRef](#)]
69. Areepak, C.; Jiradechakorn, T.; Chuetor, S.; Phalakornkule, C.; Sriariyanun, M.; Raita, M.; Champreda, V.; Laosiripojana, N. Improvement of lignocellulosic pretreatment efficiency by combined chemo–Mechanical pretreatment for energy consumption reduction and biofuel production. *Renew. Energy* **2022**, *182*, 1094–1102. [[CrossRef](#)]
70. Chen, Z.; Chen, D.; Zhao, C.; Kwan, M.P.; Cai, J.; Zhuang, Y.; Zhao, B.; Wang, X.; Chen, B.; Yang, J.; et al. Influence of meteorological conditions on PM_{2.5} concentrations across China: A review of methodology and mechanism. *Environ. Int.* **2020**, *139*, 105558. [[CrossRef](#)]
71. Chen, Z.; Xie, X.; Cai, J.; Chen, D.; Gao, B.; He, B.; Cheng, N.; Xu, B. Understanding meteorological influences on PM_{2.5} concentrations across China: A temporal and spatial perspective. *Atmos. Chem. Phys.* **2018**, *18*, 5343–5358. [[CrossRef](#)]

Disclaimer/Publisher’s Note: The statements, opinions and data contained in all publications are solely those of the individual author(s) and contributor(s) and not of MDPI and/or the editor(s). MDPI and/or the editor(s) disclaim responsibility for any injury to people or property resulting from any ideas, methods, instructions or products referred to in the content.